studies. Thus, she was diagnosed as ARDS. Pyrexia and hepatosplenomegaly were recognized again starting on day 34. The serum lactate dehydrogenase level was elevated 3 times above the normal range starting on day 36; however, serum triglycerides were within the normal range. G-CSF was discontinued on day 36. Although methylprednisolone pulse therapy, nitric oxide (NO) inhalation, and injection of pulmonary surfactant were started, her pulmonary oxygenation became worse. Finally, extracorporeal membrane oxygenation (ECMO) was started on day 38. Ferritin and soluble interleukin-2 receptor (sIL-2R) levels were 4567 ng/dL and 5842 U/mL, respectively, on day 38. The WBC count recovered to 2590/μL on day 37, but dropped to 1100/μL on day 39. Since serum ferritin was significantly elevated (273,432 ng/mL) on day 44, plasma pheresis and continuous hemodiafiltration (CHDF) were started to remove cytokines. A BM smear on day 51 was cellularly hypoplasia, but showed macrophage infiltration with active hemophagocytosis. She met 6 of the clinical criteria for a diagnosis of HLH [4] and was diagnosed as chemotherapy-related HLH. Cyclosporin A was started for HLH, but her respiratory failure did not improve and she died on day 58 due to respiratory failure. An autopsy was performed with the consent of her parents. Both lungs were diffusely hardened with reduced air content, accompanied by multiple fresh pulmonary hemorrhages. Although the hyaline membrane was only partially formed, organization of a hyaline membrane-like substance was noted, which was consistent with the findings of ARDS (Figure 1a). Histologically, no leukemic cells were present in the bone marrow, but macrophage proliferation and hemosiderin deposition were evident, which suggested that HLH

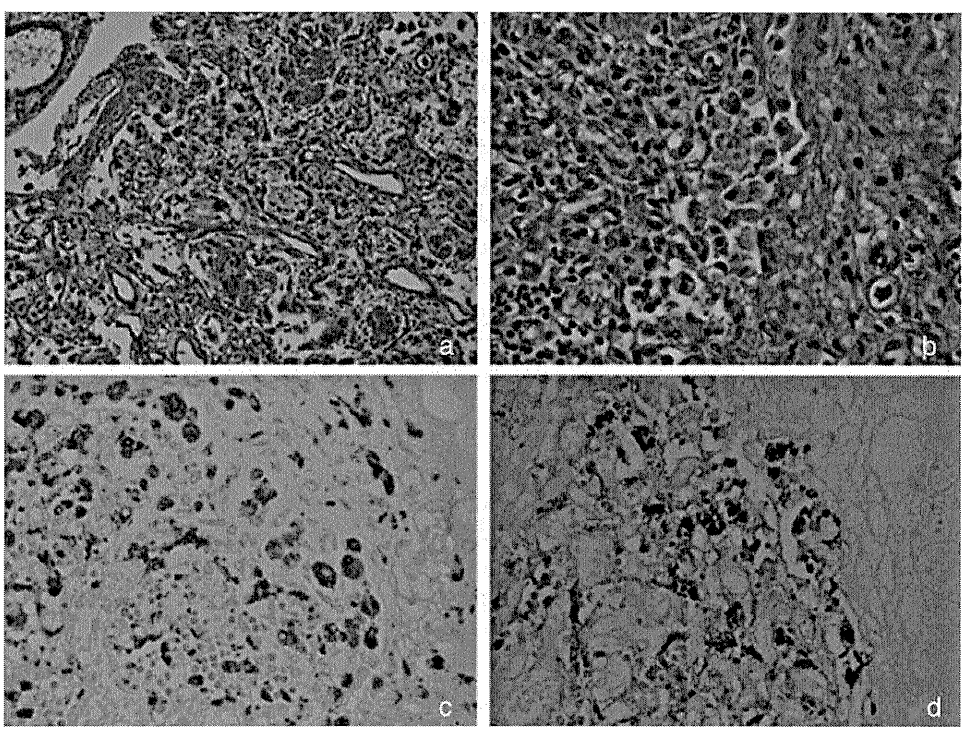

FIGURE 1 (a) Lung (hematoxylin/eosin, original magnification ×200). Although the hyaline membrane was only partially formed, organization of a hyaline membrane-like substance was noted. (b) Mesenteric lymph node (hematoxylin/eosin, original magnification ×200) shows macrophage proliferation and hemosiderin deposition. (c) Mesenteric lymph node (CD68 immunization stain, original magnification ×400) confirms the proliferation of macrophage. (d) Mesenteric lymph node (Prussian blue stain, original magnification ×400) shows hemosiderin deposition.

had developed earlier. Similar findings were noted in swollen lymph nodes over the entire body (Figure 1b–d); however, hemophagocytosis had not been noted previously.

DISCUSSION

Chemotherapy-related HLH is a very rare and lethal adverse event. It has been reported in only 4 of 971 T-cell acute lymphoblastic leukemia (T-ALL) cases in BFM-ALL trials [5], and 4 of 508 cancer children developed chemotherapy-related HLH [3]. The pathogenesis of chemotherapy-related HLH has not been proven. Intensely immunosuppressive treatment and infectious agents, such as EBV, CMV, and ADV, might have caused this complication. Another possibility is that cytokines (eg, G-CSF) might continuously stimulate the macrophage system, resulting in HLH [6]. In our case, it was possible that culture-negative severe sepsis and the prolonged administration of G-CSF were involved in the development of HLH, although the possibility of primary HLH due to a defect of the perforin (PRF1), MUNC13–4, or syntaxin 11 genes could not be excluded in our case.

It is not easy to diagnose chemotherapy-related HLH, since the clinical and laboratory presentation would resemble chemotherapy-induced myelosuppression complicated with infection. It was likely that our patient had already developed HLH on day 38, since the ferritin and sIL-2R levels were very high. Therefore, we consider retrospectively that ARDS was the initial symptom of HLH. In previous reports, some HLH patients have been diagnosed with ARDS in their clinical course. Nahum et al. [7] reported that 7 of 11 HLH children with multiple organ failure exhibited respiratory symptoms including ARDS after a diagnosis of HLH had been made. Fitzgerald and McClain [8] also reported that 10 of 25 HLH children showed alveolar-interstitial opacities with pleural effusions on chest radiographs that were compatible with ARDS. However, there is only one previous case of ARDS as a primary symptom of HLH [9]. Although we suspected HLH on day 44 when serum ferritin was extremely high, we thought that methylprednisolone pulse therapy, along with plasma pheresis and CHDF, would be enough to improve her ARDS. We did not examine BM until the WBC count dropped significantly and we did not treat HLH at that point. The onset of HLH is not easily noticed in leukemia patients, since the initial symptoms, including fever and pancytopenia, are common after chemotherapy. In fact, 11 fatal HLH cases with T-cell ALL were diagnosed to be HLH by autopsy [10]. In our case, the diagnosis based on clinical criteria was confirmed by the findings at autopsy. If her chemotherapy-related HLH had been diagnosed earlier, we may have had a chance to treat her with etoposide and dexamethasone, which are the front-line therapy for this condition [3], at an earlier stage.

For a diagnosis of chemotherapy-related HLH, bone marrow testing and the measurement of ferritin and sIL-2R are necessary, even in the pancytopenic period after chemotherapy. The possibility of HLH should be considered if patients exhibit ARDS that does not respond to supportive therapy, since more intensive treatments are necessary for HLH.

Declaration of interest

The authors report no conflicts of interest. The authors alone are responsible for the content and writing of the paper.

REFERENCES

[1] Filipovich AH. Hemophagocytic lymphohistiocytosis and other hemophagocytic disorders. *Immunol Allergy Clin N Am.* 2008;28:293–313.

[2] zur Stadt U, Beutel K, Kolberg S, et al. Mutation spectrum in children with hemophagocytic lymphohistiocytosis: molecular and functional analysis of PRF1, UNC13D, STX11, and RAB27A. *Hum Mutat.* 2006;27:62–68.
[3] Lackner H, Urban C, Sovinz P, et al. Hemophagocytic lymphohistiocytosis as severe adverse event of antineoplastic treatment in children. *Haematologica.* 2008;93:291–294.
[4] Henter JI, Horne A, Arico M, et al. HLH-2004: diagnostic and therapeutic guidelines for hemophagocytic lymphohistiocytosis. *Pediatr Blood Cancer.* 2007;48:124–131.
[5] Trebo MM, Attarbaschi A, Mann G, et al. Histiocytosis following T-acute lymphoblastic leukemia: a BFM study. *Leuk Lymphoma.* 2005;46:1735–1741.
[6] Glasser L, Legolvan M, Horwitz HM et al. Florid histiocytic hemophagocytosis following therapy with long acting G-CSF (pegfilgastim). *Am J Hematol.* 2007;82:753–757.
[7] Nahum E, Ben-Ari J, Stain J, et al. Hemophagocytic lymphohistiocytic syndrome: unrecognized cause of multiple organ failure. *Pediatr Crit Care Med.* 2000;1:51–54.
[8] Fitzgerald NE, McClain KL. Imaging characteristics of hemophagocytic lymphohistiocytosis. *Pediatr Radiol.* 2003;33:392–340.
[9] Kaneko K, Matsuda M, Sekijima Y, et al. Acute respiratory distress syndrome due to systemic lupus erythematosus with hemophagocytic syndrome: an autopsy report. *Clin Rheumatol.* 2005;24:158–161.
[10] O'Brien MM, Lee-Kim Y, George TI, et al. Precursor B-cell acute lymphoblastic leukemia presenting with hemophagocytic lymphohistiocytosis. *Pediatr Blood Cancer.* 2008;50:381–383.

J Occup Health 2011; 53: 84–92

Journal of Occupational Health

Benzene Induces Cytotoxicity without Metabolic Activation

Takuro NISHIKAWA[1,2], Kimiko IZUMO[1], Emiko MIYAHARA[1], Masahisa HORIUCHI[1], Yasuhiro OKAMOTO[2], Yoshifumi KAWANO[2] and Toru TAKEUCHI[1]

[1]Departments of Environmental Medicine and [2]Pediatrics, Graduate School of Medical and Dental Sciences, Kagoshima University, Japan

Abstract: Benzene Induces Cytotoxicity without Metabolic Activation: Takuro NISHIKAWA, *et al.* Departments of Environmental Medicine and Pediatrics, Graduate School of Medical and Dental Sciences, Kagoshima University—Objectives: Benzene has been consistently associated with hematological disorders, including acute myeloid leukemia and aplastic anemia, but the mechanisms causing these disorders are still unclear. Various metabolites of benzene lead to toxicity through the production of reactive oxygen species (ROS), the inhibition of topoisomerase and DNA damage. However, benzene itself is considered to have no mutagenic or cytotoxic activity. In this study, we investigated the effects of benzene itself on a human myeloid cell line with or without benzene metabolizing enzyme inhibitors. **Methods:** A human myeloid cell line, HL-60, was exposed to benzene with or without cytochrome P450 2E1 or myeloperoxidase inhibitor. Cytotoxicity was evaluated in terms of global DNA methylation levels, induction of apoptosis, and ROS production. **Results:** Benzene did not change global DNA methylation levels. However, benzene itself increased the levels of apoptosis and ROS. This cytotoxicity did not change with the addition of benzene metabolizing enzyme inhibitors. Benzene itself increased the mRNA levels of oxidative stress-related genes and transcription factors of activator protein-1. **Conclusions:** Benzene did not influence global DNA methylation in HL-60 cells, but had cytotoxic effects and changed gene expression levels. To elucidate the mechanisms of benzene toxicity, benzene itself as well as benzene metabolites must be investigated.
(J Occup Health 2011; 53: 84–92)

Received Oct 1, 2010; Accepted Dec 18, 2010
Published online in J-STAGE Feb 11, 2011
Correspondence to: T. Takeuchi, Department of Environmental Medicine, Graduate School of Medical and Dental Sciences, Kagoshima University, 8–35–1 Sakuragaoka, Kagoshima City, Kagoshima 890-8544, Japan
(e-mail: takeuchi@m.kufm.kagoshima-u.ac.jp)

Key words: Apoptosis, Benzene, Cytotoxicity, DNA methylation, HL-60 cells, Reactive oxygen species

Benzene is widely used for manufacturing gasoline and plastics, and is present in cigarette smoke[1]. More than four million tons of benzene are produced annually in Japan[2]. However, benzene induces bone marrow toxicity in humans, and causes hematopoietic malignancies and aplastic anemia[3]. The most frequent human malignancy associated with benzene exposure is acute myeloid leukemia (AML)[1]. The mechanism by which benzene induces leukemia and aplastic anemia has not been elucidated[1,3].

It is believed that benzene does not initiate leukemia or aplastic anemia directly. Rather, it acts through a series of benzene metabolites[4–6]. Benzene is primarily metabolized in the liver by cytochrome P450 2E1 (CYP2E1) to form reactive metabolites such as benzene oxide, catechol and hydroquinone, which can subsequently be metabolized in the bone marrow by myeloperoxidases (MPO) to produce benzoquinone metabolites [4]. Due to the complexity of benzene's metabolic pathways and the variety of its metabolites, the specific genetic and cellular changes as well as the actual metabolites involved in benzene's toxic and carcinogenic effects have not yet been identified. Since various kinds of CYP, including CYP2E1 and MPO are expressed in the human myeloid cell line HL-60[7], benzene can be metabolized in HL-60 cells.

Some reactive metabolites of benzene can undergo redox cycling, increasing the production of intracellular reactive oxygen species (ROS), which in turn may damage cellular macromolecules such as DNA, lipids, and proteins, which would lead to disruption of the cellular function[8]. Benzenetriol, hydroquinone and phenol have been shown to increase levels of 8-oxo-deoxyguanosine[9,10], a marker of oxidative DNA damage[11], in HL-60 cells, which are used as a model system for examining the proliferation and differentiation of bone marrow cells. A growing body of evidence suggests that ROS are at least partly involved in mediating the cellular effects of hydroxylated benzene

metabolites[11]. However, it is not yet clear whether benzene itself causes the generation of ROS.

Altered DNA methylation may play an important role in the pathogenesis of AML. Global DNA hypomethylation and promoter hypermethylation of tumor suppressor genes are frequently observed in hematological malignancies [12]. Recent studies have indicated that occupational exposure to low levels of benzene is associated with altered DNA methylation patterns in the peripheral blood leukocytes of gas station attendants and traffic police officers[13]. However, no previous studies have evaluated the epigenetic changes caused by benzene through the use of myeloid cell lines[14].

In this study, we examined the effects of benzene on global DNA methylation in a human myeloid cell line, HL-60. We also determined the cytotoxicity of benzene itself in HL-60 cells with the use of benzene metabolizing enzyme inhibitors, and discuss the mechanism of benzene toxicity.

Materials and Methods

Cell culture and treatments

A human myeloid cell line, HL-60, was kindly supplied by the Japanese Cancer Research Resource Bank. It was maintained in RPMI 1640 medium (SIGMA-Aldrich, St. Louis, MO) containing 10% heat-inactivated fetal calf serum (FCS) (Hyclone, Logan, UT). The cells were grown in a humidified atmosphere at 37°C in 5% CO_2. Viability was assessed by the trypan blue dye exclusion test.

Reagents

Benzene was purchased from SIGMA-Aldrich (CHROMASOLV® Plus, for HPLC, purity ≥ 99.9%) and Wako Pure Chemical (purity; 99.8%, Osaka, Japan). Chlormethiazole-HCl (CMZ) and dimethyl sulfoxide (DMSO) were purchased from SIGMA-Aldrich. 4-Aminobenzoic acid hydrazide (ABAH) was purchased from Tokyo Chemical Industry (Tokyo, Japan). H_2O_2 was purchased from Santoku Chemical Industries (Tokyo, Japan). Catalase was purchased from Boehringer-Mannheim (Mannheim, Germany) and Worthington Biochemical (Lakewood, NJ). 5-Aza-2'-deoxycytidine was purchased from Wako Pure Chemical.

Determination of 5-methyl-2'-deoxycytidine (mdC) by HPLC

HL-60 cells were suspended in RPMI-1640 containing 10% FCS at 4 × 10^5/m*l*, and benzene diluted in DMSO was then added. The final concentration of DMSO was less than 0.1%. The cells were incubated at 37°C in 5% CO_2. After being exposed to benzene for 72 h, the cells were immediately chilled in an ice-water bath, washed with ice-cold Dulbecco's phosphate buffered saline (DPBS) and then stored as cell pellets at –80°C until analysis. The cells were incubated with ribonuclease A (10 μg/sample, Nacalai Tesque, Kyoto, Japan) at 37°C for 30 min, and DNA was then extracted from the cells with a QIAamp DNA Blood Mini Kit (Qiagen, Tokyo, Japan) and enzymatically digested to nucleosides, as described elsewhere[15]. The nucleosides were separated with ODS-80TS (TOSOH, Tokyo, Japan), as described elsewhere[15]. 2'-Deoxycytidine (dC), 5-methyl-2'-deoxycytidine (mdC) and 2'-deoxyguanosine (dG) were visualized by UV/Visible detection at 280 nm. Reference standards of dC (Wako Pure Chemical), mdC (Tokyo Chemical Industry), and dG (SIGMA-Aldrich) were used. %mdC was calculated as 100 x (moles of mdC/moles of dG).

Evaluation of apoptosis by flow cytometry

HL-60 cells suspended in RPMI-1640 at 4 × 10^5/m*l* were incubated with or without benzene at 37°C in 5% CO_2 for 1 h. FCS was added to the cells at 10%, and the cells were incubated further. Benzene concentrations in the medium were reported to decrease rapidly at 37°C[16]. FCS contains proteins and lipid, and may adsorb benzene. The presence of FCS generates bubbles during the preparation of benzene solutions. To avoid any effects of FCS on apoptosis, we prepared benzene solution without FCS, incubated HL-60 cells for 1 h in the absence of FCS, and then added FCS to reduce cell damage due to the serum-free conditions[17]. After incubation, the cells were harvested by centrifugation, washed with ice-cold DPBS and fixed with 70% ethanol overnight at –20°C. The fixed cells were suspended with DPBS containing propidium iodide (PI; SIGMA-Aldrich) (15 μg/m*l*) and RNase A (50 μg/m*l*) and incubated for 30 min at 37°C in the dark. Apoptotic cells were measured using a FACScan cytometer (Becton Dickinson, Mountain View, CA) and the data were analyzed using WinMDI software version 2.9. Apoptotic cells were determined as the percentage of signals to the left of the G1 peak (sub G0/G1 population, see Fig. 2a)[18].

For the detection of phosphatidylserine as a marker of apoptosis, an Annexin V-fluorescein isothiocyanate (FITC) and PI double-labeling kit purchased from Trevigen (Gaithersburg, MD) were used, and apoptotic cells were stained according to the manufacturer's instructions. Briefly, after 8 h of exposure to benzene with or without 250 U/m*l* of catalase as described above, samples were harvested and washed, and then stained with Annexin V-FITC and PI. The cells were evaluated using FACScan, and the data were analyzed with WinMDI software version 2.9. Apoptosis was determined by evaluating the percentage of events that accumulated in the Annexin V-FITC-positive and PI-negative position (see Fig. 2c). For experiments with CMZ and ABAH, HL-60 cells were pre-incubated with RPMI1640-10% FCS containing 50 μM CMZ, 100 μM ABAH, or both CMZ (50 μM) and ABAH (100 μM) for 20 h. Cells were then suspended in RPMI-1640 containing the same concentrations of enzyme

inhibitors and exposed to 5 mM benzene. After 1 h of incubation, FCS was added to the cells to a final concentration of 10%, and the cells were incubated for 7 h. The double-staining procedures were the same as those described above.

Measurement of the intracellular generation of ROS

HL-60 cells suspended in phenol red-free RPMI-1640 at 4×10^5/m*l* were incubated with dichlorofluorescin-diacetate (DCFH-DA; Molecular Probes), as described elsewhere[19], and then exposed to 5 mM benzene with or without catalase (250 U/m*l*) for 60 min. The oxidative conversion of DCFH to dichlorofluorescein (DCF) was measured using FACScan. For experiments with CMZ, the cells were pre-treated as described above in "Evaluation of apoptosis by flow cytometry", and then suspended in phenol red-free RPMI-1640 at 4×10^5/m*l*. After the addition of the same concentration of CMZ, loaded with probes, the cells were exposed to 5 mM benzene for 60 min at 37°C. ROS levels were measured as described above.

Determination of mRNA levels by real-time PCR

Real-time PCR was used to measure the mRNA levels of epigenetic-related enzymes, and cell cycle regulatory, apoptosis-related, oxidative stress-related and transcription factor-related genes (Table 1). HL-60 cells were exposed to 5 mM benzene as described above in the section entitled "Evaluation of apoptosis by flow cytometry". Total RNA was then isolated from the cells by Trizol reagent (Invitrogen, Carlsbad, CA) according to the manufacturer's instructions. Complementary DNA was synthesized by reverse transcription from total RNA using reverse transcriptase and oligo-dT20 (Toyobo, Osaka, Japan). The resulting cDNA was amplified using the FastStart Universal SYBR Green Master (ROX) (Roche Diagnostics GmbH, Mannheim, Germany) under the following conditions: 95°C for 10 min, followed by 40 cycles of 15 s at 95°C and 1 min at 60°C. Real-time PCR was performed using a Thermal Cycler Dice® Real Time System (Takara Bio Inc., Otsu, Japan). The details of the primers used in this experiment are shown in Table 1. The relative level of mRNA was calculated using cycle time (*Ct*) values, which were normalized against the value of *GAPDH*. Relative quantification (fold change) between different samples was calculated according to the $2^{-\Delta\Delta Ct}$ method[20].

Statistical analysis

Values are shown as means ± standard error (SE). Statistical analysis was performed using StatView version 5.0 for Windows (SAS, Institute Inc., Cary, NC). Differences between groups were tested by non-parametric Wilcoxon tests. A probability value of less than 0.05 was considered to be statistically significant.

Results

Levels of global DNA methylation

In HL-60 cells exposed to 5 mM benzene, the cell number was less than in the control from 24 to 48 h (Fig. 1a). However, the levels of %mdC did not change in the presence of benzene in concentrations up to 5 mM (Fig. 1b). The levels of %mdC from 4 to 96 h of incubation also did not change (Table 2). Although the %mdC levels in HL-60 cells incubated with 1.3% DMSO did not change relative to the control, the %mdC levels with 100 μM 5-aza-2-deoxycytidine (AzaC) decreased significantly to around 1.4% compared to 4% in the control (Fig. 1c).

Levels of apoptotic cells

Figure 2b shows that the proportion of sub G0/G1 cells (corresponding to apoptotic cells, see Fig. 2a) increased among cells exposed to benzene after incubation for 4, 8 and 24 h. The induction of apoptosis by benzene was confirmed by another method. Annexin V-FITC-positive and PI-negative cells, which are considered to be apoptotic, also increased in HL-60 cells exposed to benzene alone (Fig. 2c). This increase was dependent on the benzene concentration (Fig. 2d). Since the increase at 0.05 mM and 0.5 mM was slight, albeit significant, we investigated the effects of benzene at 5 mM in later experiments. Neither CYP2E1 inhibitor (CMZ), MPO inhibitor (ABAH) nor catalase altered the levels of apoptosis induced by benzene (Fig. 2e, f).

Levels of intracellular ROS

Intracellular ROS were quantified by a flow-cytometric analysis of the ROS-sensitive fluorescent probe DCFH-DA. Fluorescence intensity was significantly increased in HL-60 cells exposed to 5 mM benzene for 60 min, and was decreased by co-incubation with catalase (Fig. 3a, b). We also investigated the effects of CMZ on ROS generation. Exposure to benzene consistently increased the fluorescence intensity (2.34 ± 0.40, mean ± SE, n=17). Exposure to benzene also increased the fluorescence intensity (1.56 ± 0.41) in cells that had been pretreated with CMZ, however, this increase was significantly less than that found in cells that were not treated with CMZ. To determine the levels of ROS by flow cytometry, we selected a presumably intact cell population by a gate (polygon in Fig. 3C). Exposure to benzene decreased the population from 80.67 ± 0.87% to 76.06 ± 1.25%. Exposure to benzene also decreased the population that had been pretreated with CMZ from 80.13 ± 1.02% to 75.55 ± 1.40%. In contrast to the generation of ROS, CMZ did not affect the decrease of the cell population induced by exposure to benzene.

Expression levels of mRNAs of various genes

We investigated the expression levels of mRNA of 30

Table 1. Primer sets used in this study

Category	Gene name	Product size (bp)	Forward primer	Reverse primer	Reference
Epigenetic systems	*DNMT1*	142	5'-GAAGAATTATCCGAGGAGGGCTA-3'	5'-GGGCTTCACTTCTTGCTTGGTT-3'	-
	DNMT3A	111	5'-ACGCCAAAGGACCCTGCGGT-3'	5'-TGGCTGGGGCTCACTCCGCT-3'	-
	DNMT3B	156	5'-TTCCCCACGTTCCACCCGAG-3'	5'-GTGAGGTCGATGGTAAGGTAAGAGC-3'	-
	HDAC1	102	5'-CAAGCTCCACATCAGTCCTTCC-3'	5'-TGCGGCAGCATTCTAAGGTT-3'	(31)
	SUVH1	115	5'-AAGAAGATCCGCGAACAGGAA-3'	5'-GGAACTGCTTGAGGATACGCAC-3'	(31)
	SUVH2	102	5'-ATCCCACCTGGTACTCCCATCT-3'	5'-GCAAAGCGAATACTGTGTGCC-3'	(31)
	EZH2	144	5'-GCGACTGAGACAGCTCAAGAGGT-3'	5'-GTCAGGATGTGCACAGGCTGT-3'	(31)
	EP300	126	5'-ATGGCCGAGAATGTGGTGGAAC-3'	5'-GTCGTGCTCCAAGTCAAATAGAG-3'	(31)
Enzyme	*TOP2A*	75	5'-AGTCGCTTTCAGGGTTCTTGAG-3'	5'-TTTCATTTACAGGCTGCAATGG-3'	(32)
	MPO	123	5'-AAGCTGCTTCTGGCCCTAGCAG-3'	5'-CTCCTCCATGGAGCTCAGCAC-3'	-
Apoptosis	*BCL2*	135	5'-GCAGAAGTCTGGGAATCGATCTG-3'	5'-TGCATAAGGCAACGATCCCATC-3'	-
	BAX	92	5'-CCTGTGCACCAAGGTGCCGG-3'	5'-GGTCTTGGATCCAGCCCAACAG-3'	-
	NOXA	153	5'-CGCGCAAGAACGCTCAACCGA-3'	5'-GCAGTCAGGTTCCTGAGCAGAAG-3'	-
	SOCS1	178	5'-GGAGCGGATGGGTGTAGGGG-3'	5'-GAGGTAGGAGGTGCGAGTTCAG-3'	(33)
Oxidative stress	*HMOX1*	119	5'-GAGGAACTTTCAGAAGGGCCAG-3'	5'-AGACTGGGCTCTCCTTGTTGCG-3'	(34)
	NQO1	119	5'-GCTCCAAGCAGCCTCTTTGAC-3'	5'-GACTTGCCCAAGTGATGGCC-3'	-
	KEAP1	121	5'-ACGGCTGCATCCACCACAACA -3'	5'-AGGAGACGATTGAGGACAGCCA-3'	-
	NFKB1	134	5'- AATGACAGAGGCGTGTATAAGG -3'	5'-GAGCTGCTTGGCGGATTAG-3'	-
	RELA	130	5'-GTTCACAGACCTGGCATCC-3'	5'-TGTCACTAGGCGAGTTATAGC-3'	(35)
	SOD1	236	5'-CATCATCAATTTCGAGCAGA -3'	5'-GCCACACCATCTTTGTCAGCAG-3'	(36)
	SOD2	181	5'-ACTGCAAGGAACAACAGGCC -3'	5'-CAGCATAACGATCGTGGTTTAC-3'	-
	CAT	188	5'-GCGGTCAAGAACTTCACTGA-3'	5'-GCTAAGCTTCGCTGCACAGGT-3'	(34)
	OGG1	145	5'-CCCCAGACCAACAAGGAACT-3'	5'-TGGAACCCTTTCTGCGCTTT-3'	(37)
	GPX1	174	5'-CCTCCCCTTACAGTGCTTGT-3'	5'-GTACCTTGCCCCGCAGGG-3'	-
AP-1	*FOS*	159	5'-CTCCGTGCCAGACATGGACCTATCT-3'	5'-GAAGACGTGTAAGCAGTGCAGCTG-3'	-
	JUN	142	5'-AAGAACTCGGACCTCCTCACCT-3'	5'-CGTTCTTGGGGCACAGGAACTG-3'	-
Cell cycle	*CDKN2A(ARF)*	87	5'-GAGAACATGGTGCGCAGGT-3'	5'-GATGTGAACCACGAAAACCCTC-3'	(38)
	CDKN2A (p16)	150	5'-ACTCTCACCCGACCCGTGCA-3'	5'-GACATCGCGATGGCCCAGCT-3'	-
	CDKN1A (p21)	146	5'-GGAAGACCATGTGGACCTGT-3'	5'-GGCGTTTGGAGTGGTAGAAA-3'	(39)
	CDKN2B (p27)	134	5'-GGAGAACAAGGGCATGCCCAG-3'	5'-TCCCGAAACGGTTGACTCCGTTG-3'	-
Internal Control	*GAPDH*	120	5'-CCATGGCACCGTCAAGGCTGA-3'	5'-ACGACGTACTCAGCGCCAGCA-3'	(40)

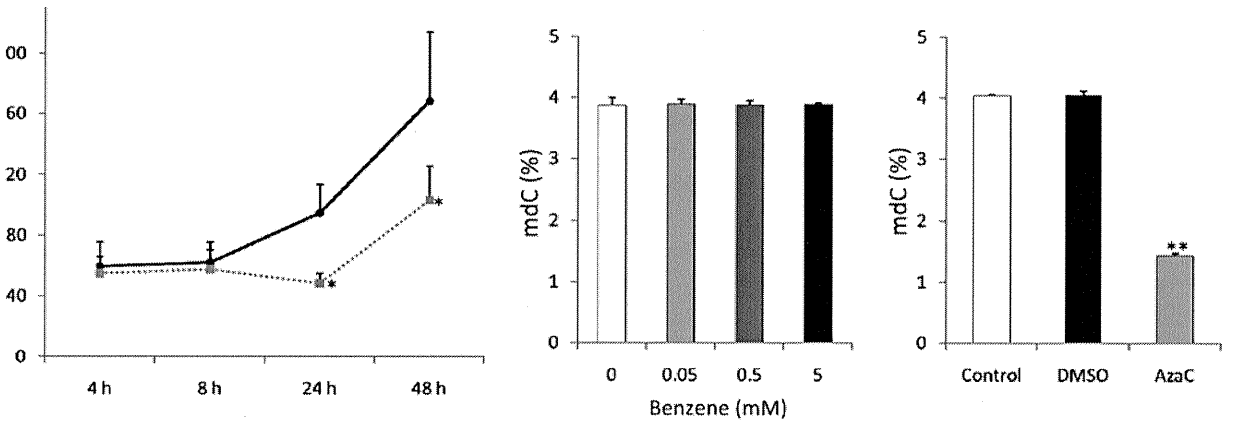

Fig. 1. Cell numbers and %mdC levels of HL-60 cells exposed to benzene and other reagents. (a) Growth of HL-60 cells and HL-60 cells exposed to benzene for up to 48 h. HL-60 cells were exposed to 5 mM benzene diluted with DMSO (■, gray line). Closed circles (●) indicate results for HL-60 cells incubated with 0.1% DMSO. (b) %mdC levels in HL-60 cells exposed to the indicated concentrations of benzene (up to 5 mM) for 72 h. (c) %mdC levels in HL-60 cells incubated for 72 h with no supplement (Control), 1.3% DMSO or 100 μM AzaC. The data are presented as means + SE values from four to eight independent experiments, except for (c). For (c), data are obtained from two independent experiments conducted in quadruplicate. %mdC was determined as described in Materials and Methods. $*p<0.05$, $**p< 0.01$ vs. Control.

Table 2. Changes in %mdC as a function of incubation time with 5 mM benzene

	4 h	8 h	24 h	48 h	96 h
DMSO	4.04 ± 0.03	4.07 ± 0.02	4.04 ± 0.03	4.07 ± 0.05	4.05 ± 0.03
Benzene	4.05 ± 0.04	4.08 ± 0.03	4.05 ± 0.06	3.99 ± 0.05	4.01 ± 0.03

Benzene was diluted with DMSO. Data are means ± S.E. from four independent experiments.

genes (Table 1) in HL-60 cells that had/had not been exposed to benzene. Among genes related to epigenetic systems such as DNA methyltransferases (Dnmts) and histone modification enzymes, only the mRNA levels of *DNMT3A* were increased 2-fold after 4 h of exposure to 5 mM benzene (Fig. 4a). The mRNA level of the genes related to cell cycle regulation and apoptosis, such as *p15, p16* and the *BCL2* protein family, were not changed by exposure to benzene (data not shown). On the other hand, mRNA levels of oxidative stress-related genes, such as *NQO1* and *HMOX1*, and transcription factor-related genes, such as *FOS* and *JUN*, increased after exposure to benzene (Fig. 4b–e).

Discussion

Benzene, an important industrial chemical and a ubiquitous environmental pollutant, is an established carcinogen and myelotoxicant. Epidemiological studies have found that, exposure to benzene is associated with the development of AML and aplastic anemia in humans. However, the mechanism by which benzene induces hematological disorders has not been elucidated[1, 3].

Recently, altered DNA methylation has been suggested in epidemiological studies to be one of the potential mechanisms underlying the leukemogenesis associated with benzene[13]. Global DNA hypomethylation may play an important role in human leukemogenesis contributing to carcinogenesis through the generation of chromosomal instability, reactivation of transposable elements, and loss of imprinting[21]. Ji *et al.* reported that hydroquinone, a metabolite of benzene, induced global DNA hypomethylation in TK6 lymphoid cells[14]. However, in our study, benzene did not induce global DNA hypomethylation at all (Fig. 1b). In addition, after cells were exposed to benzene for 4, 8, 24, 48, and 96 h, %mdC levels were not changed (Table 2). The difference in the cell lines used for the experiments may explain these conflicting results. Other possible explanations are the differences in the hydroquinone concentrations used in the experiments or the co-existence of other metabolites in our experiment. Since we tried to elucidate the carcinogenic mechanism of benzene in AML, we investigated the DNA methylation status after exposure to benzene in a myeloid cell line, HL-60 . The mRNA level of *DNMT3A*, which causes *de novo* DNA methylation, increased about 2-fold after 4 h of exposure to benzene

(Fig. 4a). This finding suggests that benzene may affect the epigenetic profile, such as promoter hypermethylation of tumor suppressor genes, but not global DNA methylation. The %mdC levels in HL-60 cells in our experiments are similar to those reported earlier by Aarbakke, *et al.*[22] and decreased when cells were incubated with AzaC.

It is generally accepted that benzene toxicity is mediated through the metabolic formation of reactive metabolites [3–6]. Various metabolites of benzene are considered to lead to toxicity through the production of ROS, inhibition of topoisomerase and induction of DNA damage[3–6]. We investigated whether benzene itself is actually cytotoxic. Through the use of two different methods, we confirmed that benzene induced apoptosis in HL-60 cells. Benzene increased the sub G0/G1 fraction and Annexin V-FITC-positive/PI-negative cells after 8 h of exposure (Fig. 2). We then investigated whether this action of benzene was due to its metabolites. We pretreated HL-60 cells with CMZ, ABAH or both CMZ and ABAH, and then exposed the treated cells to benzene in the presence of inhibitors. These inhibitors did not change the levels of apoptosis induced by benzene. This finding suggests that benzene itself induced apoptosis in HL-60 cells. To exclude the possibility that contaminants in the benzene preparation increased the levels of apoptosis, we used two benzene preparations from two different manufacturers with different purities (99.8 and 99.9%). At the same benzene concentration, the benzene preparations showed similar results, indicating that benzene itself, rather than any contaminants, induced apoptosis. Figure 2b shows that the proportion of sub G0/G1 cells decreased as incubation proceeded. Slight apoptosis may occur in HL-60 cells at the time of exposure to benzene due to incubation without FCS and mechanical stirring. Such apoptotic cells may be lost or degraded further during incubation.

Benzene metabolites have been reported to generate ROS in HL-60 cells[10], and ROS induce apoptosis in various cell lines[8,9]. Therefore, we determined intracellular ROS levels by flow cytometry with DCFH . Non-fluorescent DCFH has been reported to change to fluorescent DCF upon reaction with H_2O_2 and peroxidases[23]. Exposure to benzene increased the fluorescence of HL-60 cells and this fluorescence was decreased by the addition of catalase. Even though HL-60 cells were pretreated with CMZ, the fluorescence intensity increased in HL-60 cells exposed to 5 mM benzene. This finding indicates that benzene itself generated ROS in HL-60 cells. Although CMZ partially inhibited the generation of ROS caused by exposure to benzene, CMZ did not inhibit apoptosis or the decrease of a presumably intact cell population. While benzene metabolites might be involved in generation of ROS, we consider the cytotoxicity seen in our experiments to be caused by benzene itself rather than by any benzene metabolites. Catalase, which decreased the levels of ROS induced by benzene, did not suppress the level of apoptosis induced by benzene. Therefore, ROS might not be a trigger of apoptosis in HL-60 cells exposed to benzene. Although frequently used solvents, including DMSO and ethanol, did not induce apoptosis in HL-60 cells (data not shown), lipophilic solvents such as benzene might cause apoptosis due to a direct effect on the cellular membrane. We are planning to explore whether other lipophilic solvents induce apoptosis in human cell lines.

Since benzene itself increased the levels of ROS in HL-60 cells, we studied the expression levels of genes of a redox-sensitive signaling pathway by real-time PCR. Exposure of HL-60 cells to benzene resulted in a remarkable increase in oxidative stress-related genes (*HMOX1* and *NQO1*) (Fig. 4b, c) and transcription factor (*FOS* and *JUN*) mRNA levels (Fig. 4d, e). *HMOX1* and *NQO1* act as intracellular antioxidant molecules regulated by Nrf-2 (NF-E2 related factor-2)[24]. *FOS* and *JUN* belong to the AP-1 (activator protein) family, which regulates gene expression in response to a variety of stimuli, including cytokines, growth factors, and stress. AP-1 in turn controls several cellular processes including differentiation, proliferation, and apoptosis[25]. Activation of the *FOS* gene has been especially associated with the promotion of neoplastic transformation[25]. In our study, mRNA levels of NFκB signaling-related genes did not increase. This may have been because the oxidative stress that is induced by benzene is only weak, or specifically activates Nrf-2 and AP-1 signaling. Depending on the level of ROS, different redox-sensitive transcription factors are activated and coordinate distinct biological responses. The expression levels of genes change due to mechanical stress[26, 27], and may be modulated by changes in the CO_2 concentration or pH under exposure to benzene. Such effects may remain and induce large variations, especially in experiments with 4 h of incubation. We did not investigate the changes in gene expression levels in CMZ-pretreated cells because CMZ itself may affect gene expression levels[28].

The concentrations of benzene used in this study were relatively high. However, 5 mM benzene corresponds to 0.045% (v/v) and 395 ppm. Aksoy reported that benzene concentrations in workplaces were 210 to 650 ppm and those in adhesives and thinners were between 9 and 88%[29]. In a C57B1/6 mouse experiment, the incidence of leukemia was increased after exposure to benzene at 300 ppm[30]. Therefore, our benzene concentrations were similar to those that have been shown to lead to the development of leukemia after long-term exposure.

Conclusion

While benzene had no influence on global DNA methylation levels in HL-60 cells, benzene itself induced cytotoxic effects and changes in gene expression levels. To better understand the mechanisms that underlie the

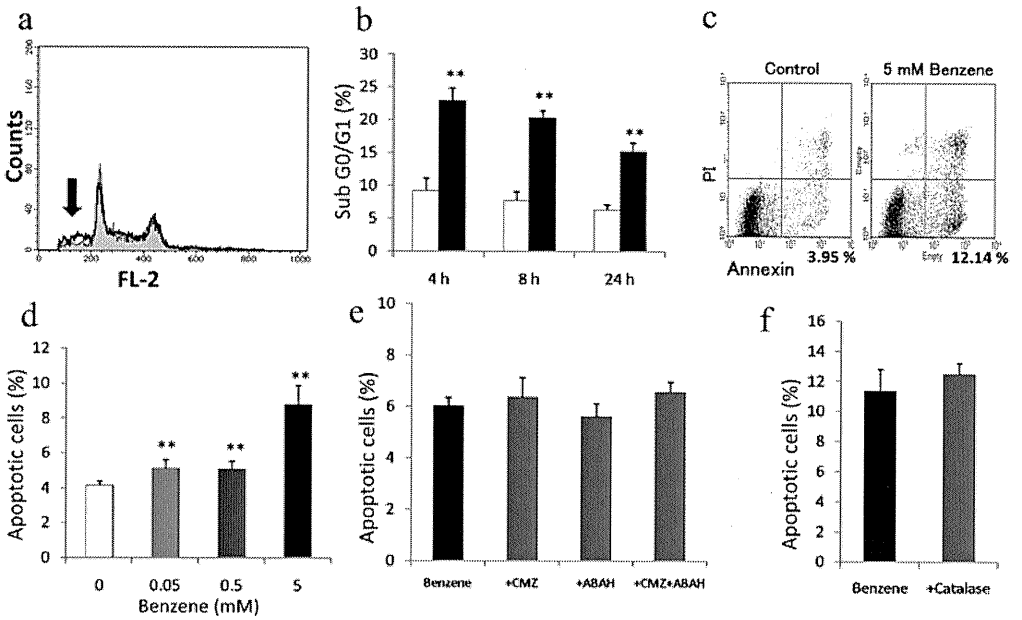

Fig. 2. Proportion of apoptotic cells in HL-60 cells exposed to benzene and other reagents. (a) Representative histograms of ethanol-fixed and PI-stained HL-60 cells exposed to 0 (filled gray line) or 5 mM benzene (black line) for 8 h. Benzene was diluted directly with RPMI-1640, and HL-60 cells were exposed to 0 or 5 mM benzene in RPMI-1640 for 1 h. Next, FCS was added to the HL-60 cells at 10%. PI staining was carried out as described in Materials and Methods. The arrow shows the sub G0/G1 phase. (b) The percentage of cells in the sub G0/G1 phase was measured in HL-60 cells (□) and HL-60 cells exposed to 5 mM benzene (■) for 4, 8 and 24 h. The exposure conditions were the same as those described above. (c) Representative dot grams of HL-60 cells (left) and HL-60 cells exposed to 5 mM benzene (right) for 8 h. HL-60 cells were double-stained with Annexin V-FITC and PI as described in Material and Methods. Cells in the lower right quadrant, which were stained with Annexin V-FITC but not PI, were considered to be apoptotic. The percentages of cells in the lower right quadrant are listed. The exposure conditions were the same as those described above. (d) Percentages of apoptotic cells in HL-60 cells and HL-60 cells exposed to benzene (up to 5 mM) for 8 h. The exposure conditions and double-staining procedures were the same as those described above. (e) Percentages of apoptotic cells in HL-60 cells exposed to 5 mM benzene for 8 h in the presence of enzyme inhibitors. HL-60 cells were incubated with RPMI1640-10% FCS containing 50 μM CMZ (CYP2E1 inhibitor), 100 μM ABAH (MPO inhibitor), or both CMZ (50 μM) and ABAH (100 μM) for 20 h. Cells were then suspended in RPMI-1640 containing the same concentrations of enzyme inhibitors and exposed to 5 mM benzene. After 1 h of incubation, FCS was added to the cells at 10%, and the cells were incubated for 7 h. The double-staining procedures were the same as those described above. (f) Percentages of apoptotic cells in HL-60 cells exposed to 5 mM benzene for 8 h with or without 250 U/m*l* of catalase (H_2O_2 scavenger). The exposure conditions and double-staining procedures were the same as those described above. The data are presented as means + SE from three to eight independent experiments. $^{**}p<0.01$ vs. HL-60 cells that were not exposed to benzene in the corresponding condition.

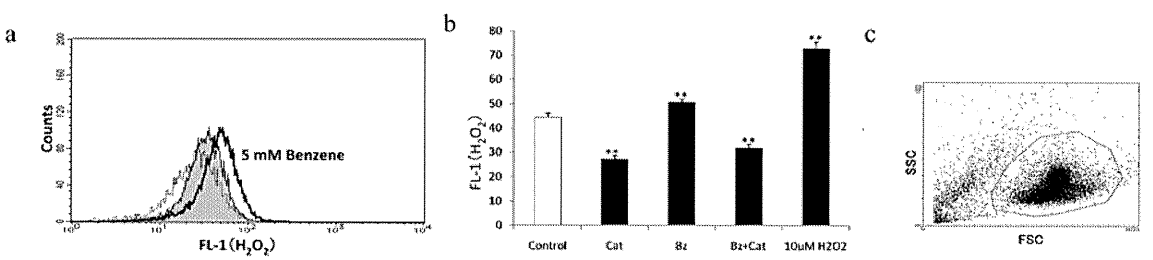

Fig. 3. Levels of intracellular ROS after exposure to benzene.(a) Representative histograms of HL-60 cells exposed to nothing (gray, filled), 5 mM benzene (black bold line) or 5 mM benzene with 250 U/m*l* catalase (dotted line) . Intracellular ROS levels were quantified using flow-cytometry analysis with the ROS-sensitive fluorescent probe DCFH-DA as described in Materials and Methods. (b) Fluorescence intensities of HL-60 cells exposed to nothing (Cont), catalase (Cat), 5 mM benzene (Bz), 5 mM benzene and catalase (Bz+Cat) or 10 μM H_2O_2 (■) for 60 min. ROS levels were measured as described above. (c) A representative dot gram of HL-60 cells. To analyze ROS in cells, we selected presumably intact cells with a polygon. The data are presented as means + SE of three independent experiments conducted in duplicate. $^{**}p<0.01$ vs. Control.

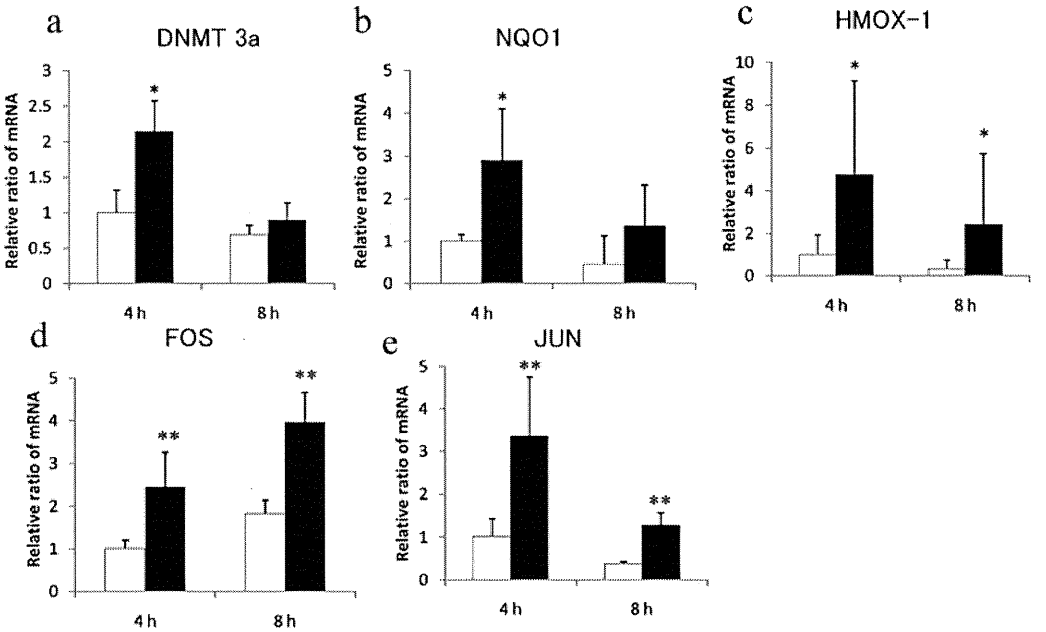

Fig. 4. Expression levels of mRNA of various genes in HL-60 cells exposed to benzene. HL-60 cells were exposed to nothing (□) or 5 mM benzene (■) for 4 or 8 h as described in the text and the legend for Fig. 2(a). The mRNA levels of an epigenetic systems-related gene (*DNMT3A*), oxidative stress-related genes (*NQO1, HMOX1*), and transcription factor-related genes of the AP-1 family (*FOS, JUN*) were determined as described in Materials and Methods. The relative values for the respective mRNA in HL-60 cells without exposure at 4 h were set to 1.0. The data are presented as means + SE of five independent experiments. $*p<0.05$, $**p<0.01$ vs. HL-60 cells that were not exposed to benzene in the corresponding condition.

toxic and carcinogenic effects of benzene, we should investigate the effects of benzene itself as well as those of benzene metabolites.

Acknowledgments: This study was supported in part by a Grant-in-Aid for Challenging Exploratory Research from the Ministry of Education, Culture, Sports, Science and Technology of Japan (#21659158), by JKA through its promotion funds from KEIRIN RACE, and by the Morinaga Foundation for Health & Nutrition.

References

1) Huff J. Benzene-induced cancers: abridged history and occupational health impact. Int J Occup Environ Health 2007; 13: 213–21.
2) Chemical Industry Statistics by the Ministry of Economy, Trade and Industry. [Online]. 2010 [cited 2010 Aug 31]; Available from: URL: http://www.meti.go.jp/statistics/tyo/seidou/result/ichiran/02_kagaku.html (in Japanese).
3) Whysner J, Reddy MV, Ross PM, Mohan M, Lax EA. Genotoxicity of benzene and its metabolites. Mutat Res 2004; 566: 99–130.
4) Snyder R, Hedli CC. An overview of benzene metabolism. Environ Health Perspect 1996; 104 (Suppl. 6): 1165–71.
5) Golding BT, Watson WP. Possible mechanisms of carcinogenesis after exposure to benzene. In: Singer B, Bartsch H, Editors. Exocyclic DNA Adducts in Mutagenesis and Carcinogenesis. Lyon (France): IARC Scientific Publications, 1999. p. 75–88.
6) Ross D. The role of metabolism and specific metabolites in benzene-induced toxicity: evidence and issues . J Toxicol Environ Health 2000; 61: 357–72.
7) Nagai F, Hiyoshi Y, Sugimachi K, Tamura H. Cytochrome P450 (CYP) expression in human myeloblastic and lymphoid cell lines. Biol Pharm Bull 2002; 25: 383–5.
8) Snyder R. Benzene's toxicity: a consolidated short review of human and animal studies by HA Khan. Hum Exp Toxicol 2007; 26: 687–96.
9) Kolachana P, Subrahmanyam VV, Meyer KB, Zhang L, Smith MT. Benzene and its phenolic metabolites produce oxidative DNA damage in HL60 cells in vitro and in the bone marrow in vivo. Cancer Res 1993; 53: 1023–26.
10) Zhang L, Robertson ML, Kolachana P, Davison AJ, Smith MT. Benzene metabolite, 1,2,4-benzenetriol, induces micronuclei and oxidative DNA damage in human lymphocytes and HL60 cells. Environ Mol Mutagen 1993; 21: 339–48.
11) Subrahmanyam V, Ross D, Eastmond D, Smith MT. Potential role of free radicals in benzene-induced myelotoxicity and leukemia. Free Radic Biol Med 1991; 11: 495–515.

12) Esteller M. Profiling aberrant DNA methylation in hematologic neoplasms: a view from the tip of the iceberg. Clin Immunol 2003; 109: 80–8.
13) Bollati V, Baccarelli A, Hou L, et al. Changes in DNA methylation patterns in subjects exposed to low-dose benzene. Cancer Res 2007; 67: 876–80.
14) Ji Z, Zhang L, Peng V, Ren X, McHale CM, Smith MT. A comparison of the cytogenetic alterations and global DNA hypomethylation induced by the benzene metabolite, hydroquinone, with those induced by melphalan and etoposide. Leukemia 2010; 24: 986–91.
15) Takeuchi T, Nakajima M, Ohta Y, Mure K, Takeshita T, Morimoto K. Evaluation of 8-hydroxydeoxyguanosine, a typical oxidative DNA damage, in human leukocytes. Carcinogenesis 1994; 15: 1519–23.
16) Giuliano M, Stellavato A, Cammarota M, et al. Effects of low concentrations of benzene on human lung cells in vitro. Toxicol Lett 2009; 188: 130–6.
17) Simoni D, Giannini G, Roberti M, et al. Studies on the apoptotic activity of natural and synthetic retinoids: discovery of a new class of synthetic terphenyls that potently support cell growth and inhibit apoptosis in neuronal and HL-60 cells. J Med Chem 2005; 48: 4293-9.
18) Nicoletti I, Migliorati G, Pagliacci MC, Grignani F, Riccardi C. A rapid and simple method for measuring thymocyte apoptosis by propidium iodide staining and flow cytometry. J Immunol Methods 1991; 139: 271–9.
19) Takeuchi T, Nakajima M, Morimoto K. Relationship between the intracellular reactive oxygen species and the induction of oxidative DNA damage in human neutrophil-like cells. Carcinogenesis 1996; 17: 1543–8.
20) Livak KJ, Schmittgen TD. Analysis of relative gene expression data using real-time-quantitative PCR and the $2^{-\Delta\Delta Ct}$ method. Methods 2001; 25: 402–8.
21) Rodriguez J, Frigola J, Vendrell E, et al. Chromosomal instability correlates with genome-wide DNA demethylation in human primary colorectal cancers. Cancer Res 2006; 66: 8462–8.
22) Aarbakke J, Miura GA, Prytz PS, et al. Induction of HL-60 cell differentiation by 3-deaza-(±)-aristeromycin, an inhibitor of S-adenosylhomocysteine hydrolase. Cancer Res 1986; 46: 5469–72.
23) Bass DA, Parce JW, Dechatelet LR, Szejda P, Seeds MC, Thomas M. Flow cytometric studies of oxidative product formation by neutrophils: a graded response to membrane stimulation. J Immunol 1983; 130: 1910–7.
24) Surh YJ, Kundu JK, Na HK, Lee JS. Redox-sensitive transcription factors as prime targets for chemoprevention with anti-inflammatory and antioxidative phytochemicals. J Nutr 2005; 135: 2993S–3001S.
25) Angel P, Karin M. The role of jun, fos and the AP-1 complex in cell-proliferation and transformation. Biochim Biophys Acta 1991; 1072: 129–57.
26) Ali F, Zakkar M, Karu K, et al. Induction of the cytoprotective enzyme heme oxygenase-1 by statins is enhanced in vascular endothelium exposed to laminar shear stress and impaired by disturbed flow. J Biol Chem 2009; 284: 18882–92.
27) Warabi E, Takabe W, Minami T, et al. Shear stress stabilizes NF-E2-related factor 2 and induces antioxidant genes in endothelial cells: role of reactive oxygen/nitrogen species. Free Radic Biol Med 2007; 42: 260–9.
28) Hu Y, Mishin V, Johansson I, et al. Chlormethiazole as an efficient inhibitor of cytochrome P450 2E1 expression in rat liver. J Pharmacol Exp Ther 1994; 269: 1286–91.
29) Aksoy M. Hematotoxicity and carcinogenicity of benzene. Environ Health Perspect 1989; 82: 193–7.
30) Cronkite EP, Bullis J, Inoue T, Drew RT. Benzene inhalation produces leukemia in mice. Toxicol Appl Pharmacol 1984; 75: 358–61.
31) Hu N, Qiu X, Luo Y, et al. Abnormal histone modification patterns in lupus CD4+ T cells. J Rheumatol 2008; 35: 804–10.
32) Wang YH, Takanashi M, Tsuji K, et al. Level of DNA topoisomerase II alpha mRNA predicts the treatment response of relapsed acute leukemic patients. Leuk Res 2009; 33: 902–7.
33) Xu SB, Liu XH, Li BH, et al. DNA methylation regulates constitutive expression of Stat6 regulatory genes SOCS-1 and SHP-1 in colon cancer cells. J Cancer Res Clin Oncol 2009; 135: 1791–8.
34) Monzen S, Takahashi K, Yoshino H, et al. Heavy ion beam irradiation regulates the mRNA expression in megakaryocytopoiesis from human hematopoietic stem/progenitor cells. J Radiat Res 2009; 50: 477–86.
35) Xiao M, Inal CE, Parekh VI, Li XH, Whitnall MH. Role of NF-kB in hematopoietic niche function of osteoblasts after radiation injury. Exp Hematol 2009; 37: 42–64.
36) Cornejo-Garcia JA, Mayorga C, Torres MJ, et al. Anti-oxidant enzyme activities and expression and oxidative damage in patients with non-immediate reactions to drugs. Clin Exp Immunol 2006; 145: 287–95.
37) Zhoua F, Zhanga W, Wei Y, et al. The changes of oxidative stress and human 8-hydroxyguanine glycosylase1 gene expression in depressive patients with acute leukemia. Leuk Res 2007; 31: 387–93.
38) Kanao H, Enomoto T, Ueda Y, et al. Correlation between p14 ARF/p16 INK4A expression and HPV infection in uterine cervical cancer. Cancer Lett 2004; 213: 31–7.
39) Mizuno S, Bogaard HJ, Voelkel NF, et al. Hypoxia regulates human lung fibroblast proliferation via p53-dependent and -independent pathways. Respir Res 2009; 10:17.
40) Izumo K, Horiuchi M, Komatsu M, et al. Dehydroepiandrosterone increased oxidative stress in a human cell line during differentiation. Free Radic Res 2009; 43: 922–31.

Benzene Metabolite 1,2,4-Benzenetriol Induces Halogenated DNA and Tyrosines Representing Halogenative Stress in the HL-60 Human Myeloid Cell Line

Takuro Nishikawa,[1,2] Emiko Miyahara,[1] Masahisa Horiuchi,[1] Kimiko Izumo,[1] Yasuhiro Okamoto,[2] Yoshichika Kawai,[3] Yoshifumi Kawano,[2] and Toru Takeuchi[1]

[1]Department of Environmental Medicine, and [2]Department of Pediatrics, Graduate School of Medical and Dental Sciences, Kagoshima University, Kagoshima, Japan; [3]Laboratory of Food and Biodynamics, Graduate School of Bioagricultural Sciences, Nagoya University, Nagoya, Japan

BACKGROUND: Although benzene is known to be myelotoxic and to cause myeloid leukemia in humans, the mechanism has not been elucidated.

OBJECTIVES: We focused on 1,2,4-benzenetriol (BT), a benzene metabolite that generates reactive oxygen species (ROS) by autoxidation, to investigate the toxicity of benzene leading to leukemogenesis.

METHODS: After exposing HL-60 human myeloid cells to BT, we investigated the cellular effects, including apoptosis, ROS generation, DNA damage, and protein damage. We also investigated how the cellular effects of BT were modified by hydrogen peroxide (H_2O_2) scavenger catalase, hypochlorous acid (HOCl) scavenger methionine, and 4-aminobenzoic acid hydrazide (ABAH), a myeloperoxidase (MPO)-specific inhibitor.

RESULTS: BT increased the levels of apoptosis and ROS, including superoxide ($O_2^{\bullet-}$), H_2O_2, HOCl, and the hydroxyl radical ($^{\bullet}OH$). Catalase, ABAH, and methionine each inhibited the increased apoptosis caused by BT, and catalase and ABAH inhibited increases in HOCl and $^{\bullet}OH$. Although BT exposure increased halogenated DNA, this increase was inhibited by catalase, methionine, and ABAH. BT exposure also increased the amount of halogenated tyrosines; however, it did not increase 8-oxo-deoxyguanosine.

CONCLUSIONS: We suggest that BT increases H_2O_2 intracellularly; this H_2O_2 is metabolized to HOCl by MPO, and this HOCl results in possibly cytotoxic binding of chlorine to DNA. Because myeloid cells copiously express MPO and because halogenated DNA may induce both genetic and epigenetic changes that contribute to carcinogenesis, halogenative stress may account for benzene-induced bone marrow disorders and myeloid leukemia.

KEY WORDS: benzene, hypochlorous acid, leukemia, myeloperoxidase, reactive oxygen species. *Environ Health Perspect* 120:62–67 (2012). http://dx.doi.org/10.1289/ehp.1103437 [Online 22 August 2011]

Benzene, widely used in the chemical industry, is a common environmental contaminant found in gasoline, cigarette smoke, and coal tar. In humans, chronic exposure to benzene results in progressive deterioration in hematopoiesis, possibly leading to myelodysplastic syndrome and acute myeloid leukemia (Aksoy 1989; Huff 2007).

Although the mechanisms of benzene toxicity remain unclear, it is considered to occur only after metabolic activation (Snyder and Hedli 1996; Whysner et al. 2004). In the liver, benzene is primarily metabolized by cytochrome P450 2E1 (CYP2E1) to benzene oxide, which is then converted by epoxide hydrolase to dihydrodiol. Subsequent processing by dihydrodiol dehydrogenase yields catechol (CT). Alternatively, by nonenzymatic rearrangement, benzene oxide is converted to phenol, which can be oxidized by CYP2E1 to 1,4-hydroquinone (HQ) and 1,4-benzoquinone (Snyder and Hedli 1996). The pathway for formation of 1,2,4-benzenetriol (BT) in humans is not yet clearly understood; it has been suggested that BT may be formed by the hydroxylation of either HQ or CT (Henderson et al. 1989; Inoue et al. 1989).

Various metabolites of benzene are considered to bring out toxicity through the generation of reactive oxygen species (ROS), inhibition of topoisomerase, and subsequent induction of DNA damage (Whysner et al. 2004). Among benzene metabolites, the triphenolic metabolite BT reacts most actively with molecular oxygen (Lewis et al. 1988; Zhang et al. 1996). We also know that BT induces oxidative DNA damage and breaks DNA strands (Kawanishi et al. 1989; Kolachana et al. 1993; Lewis et al. 1988). Moreover, BT damages DNA more severely than does HQ, and benzene and CT per se have no detectable effects on DNA (Kawanishi et al. 1989). Because epidemiological studies of HQ and 1,4-benzoquinone have never demonstrated carcinogenicity in humans, the International Agency for Research on Cancer (IARC) assigned their carcinogenic risk to humans as group 3: not classifiable as to carcinogenicity to humans (IARC 2011). Meanwhile, IARC has not evaluated the carcinogenicity of BT.

The heme enzyme myeloperoxidase (MPO), which is synthesized and secreted by neutrophils, monocytes, and other myeloid cells, is an important source of oxidants. MPO catalyzes the formation of hypochlorous acid (HOCl), a powerful oxidant derived from chloride ions and hydrogen peroxide (H_2O_2). HOCl is a potent cytotoxin that plays key roles in host defense by oxidizing the cellular constituents of invading pathogens (Hurst and Barrette 1989). At the same time, HOCl is also capable of damaging proteins, lipids, and nucleic acids in host tissue (Heller et al. 2000). By damaging the DNA of host cells, MPO-induced DNA halogenation might contribute to the association between chronic inflammation and cancer (Marnett 2000).

Although benzene is known to be specifically toxic to bone marrow in humans, the mechanism for this is not understood (Whysner et al. 2004). MPO has a much higher endogenous presence in bone marrow than in any other internal organ (Heller et al. 2000), but no previous study has examined the role of MPO-derived HOCl in benzene toxicity.

We investigated the effect of MPO-derived HOCl on the toxicity of BT in the HL-60 human myeloid cell line. To examine DNA damage induced by BT, we used an immunocytometric method to evaluate halogenated DNA, and we determined 8-oxo-deoxyguanosine (8-oxo-dG) levels using high-performance liquid chromatography (HPLC) coupled with electrochemical detection (ECD). We found that BT generates HOCl via the H_2O_2–MPO–halide system; rather than generating 8-oxo-dG, this HOCl halogenates DNA.

Materials and Methods

Cell culture. The HL-60 human promyelocytic leukemia cell line was kindly supplied by the Japanese Cancer Research Resource Bank (Osaka, Japan). Cells were maintained

Address correspondence to T. Nishikawa, Department of Environmental Medicine, Kagoshima University Graduate School of Medical and Dental Sciences, 8-35-1 Sakuraga-oka, Kagoshima, 890-8544, Japan. Telephone: 81–99-275-5288. Fax: 81–99-265-8434. E-mail: adu44150@ams.odn.ne.jp

We thank D. Eunice for copyediting the manuscript.

This study was supported in part by a Grant-in-Aid for Challenging Exploratory Research from the Ministry of Education, Culture, Sports, Science and Technology of Japan (21659158) and by the Morinaga Foundation for Health and Nutrition.

The authors declare they have no actual or potential competing financial interests.

Received 12 January 2011; accepted 22 August 2011.

in RPMI 1640 medium (Sigma-Aldrich, St. Louis, MO, USA) containing 10% heat-inactivated fetal calf serum (FCS; Hyclone, Logan, UT, USA) at 37°C in a humidified atmosphere with 5% carbon dioxide (CO_2).

Reagents. We purchased BT, HQ, and CT from Wako Pure Chemical Industries (Osaka, Japan); catalase from Boehringer-Mannheim (Mannheim, Germany); 4-aminobenzoic acid hydrazide (ABAH) from Tokyo Chemical Industry (Tokyo, Japan); and methionine and sodium hypochlorite (NaOCl) from Nacalai Tesque (Kyoto, Japan).

Determination of apoptosis by flow cytometry. We used annexin V–fluorescein isothiocyanate (FITC) and propidium iodide (PI) double-labeling kits (TACS Annexin V-FITC Kit; Trevigen, Gaithersburg, MD, USA) to detect phosphatidylserine as a marker of apoptosis. HL-60 cells suspended in RPMI 1640/10% FCS at 4×10^5/mL were exposed to BT (25–100 μM) at 37°C in 5% CO_2 for 8 hr. For experiments with catalase (H_2O_2 scavenger), cells were exposed to BT plus 250 U/mL catalase. For experiments with ABAH (MPO inhibitor) and methionine (HOCl scavenger), HL-60 cells were preincubated with RPMI 1640/10% FCS containing 100 μM ABAH or 25 mM methionine for 24 hr; media was then replaced with new media containing the reagent plus BT. Unexposed HL-60 cells were used as controls. After incubation, cells were harvested and washed and then stained with annexin V–FITC and PI according to the manufacturer's instructions. We evaluated the cells using a FACScan flow cytometer (Becton Dickinson, Mountain View, CA, USA), and data were analyzed using WinMDI software (version 2.9; Biology Software Net, La Habra, CA, USA).

Determination of intracellular ROS generation by flow cytometry. To detect intracellular superoxide ($O_2^{\bullet-}$) and H_2O_2, we followed the method of Takeuchi et al. (1996). Briefly, HL-60 cells suspended in phenol-red–free RPMI 1640 at 4×10^5/mL were incubated with hydroethidine (HE; Molecular Probes, Carlsbad, CA, USA) or dichlorofluorescin-diacetate (DCFH-DA; Molecular Probes). The probe-loaded cells were then exposed to BT with or without 250 U/mL catalase for 30 min at 37°C. For experiments with ABAH or methionine, the cells were pretreated as described above and then suspended in phenol-red–free RPMI 1640 at 4×10^5/mL. After addition of the same concentration of ABAH or methionine, loaded with probes, the cells were exposed to BT for 30 min at 37°C. Nonfluorescent HE is oxidized to fluorescent 2-hydroxyethidium by $O_2^{\bullet-}$, whereas DCFH is oxidized to dichlorofluorescein (DCF) by H_2O_2 and peroxidases (Rothe and Valet 1990). Presence of 2-hydroxyethidium or DCF was measured by FACScan.

For selective detection of HOCl and the hydroxyl radical (•OH), HL-60 cells suspended in phenol-red-free–RPMI 1640 at 4×10^5/mL were incubated with 10 μM aminophenyl fluorescein (APF; Sekisui Medical, Tokyo, Japan) or 10 μM hydroxyphenyl fluorescein (HPF; Sekisui Medical) and then exposed to BT for 30 min at 37°C with or without 250 U/mL catalase. For experiments with ABAH or methionine, cells were pretreated and exposed as described above. APF and HPF themselves are not highly fluorescent, but when reacted with HOCl (APF) or •OH (HPF) they exhibit strong dose-dependent fluorescence, which can be used to differentiate HOCl and •OH from H_2O_2, nitric oxide, and $O_2^{\bullet-}$ (Setsukinai et al. 2003). The specificity and usefulness of these probes have been described previously (Kohanski et al. 2007; Nakazato et al. 2007). We measured the fluorescence intensity of cells by FACScan and analyzed data using WinMDI software.

Determination of halogenated DNA by immunocytometric analysis. To detect DNA damage by HOCl, we analyzed halogenated DNA using a novel monoclonal antibody (mAb2D3) that recognizes the HOCl-modified 2′-deoxycytidine residue 5-chloro-2′-deoxycytidine (5-CldC; supplied by Y. Kawai, Nagoya University, Nagoya, Japan) (Kawai et al. 2004, 2008). HL-60 cells were suspended in RPMI 1640/10% FCS at 1×10^6/mL and then exposed to 50 μM BT with or without catalase. For experiments with ABAH or methionine, cells were pretreated as described above and then exposed to BT for 1 hr or 4 hr at 37°C in 5% CO_2. HL-60 cells were exposed to 20 μM HQ or 1 mM NaOCl for 1 hr or 4 hr at 37°C in 5% CO_2. After exposure, the cells were washed with phosphate-buffered saline (PBS) and then fixed in 4% paraformaldehyde (Wako Pure Chemical) at 4°C for 20 hr. We evaluated halogenated DNA as described elsewhere (Kawai et al. 2004, 2008), with minor modifications. Briefly, the fixed cells were permeabilized by a 3-min exposure, on ice, to PBS containing 0.3% Triton X-100. The cells were then blocked with 2% bovine serum albumin (Sigma-Aldrich) in PBS containing 0.05% Tween 20 (TPBS). The cells were then incubated with mAb2D3 in TPBS for 1 hr at room temperature. After washing with TPBS, the cells were incubated in TPBS for 1 hr at room temperature with FITC-labeled anti-mouse IgG (Dako, Kyoto, Japan). After incubation, cells were washed with TPBS and their fluorescence intensity was measured by FACScan. The data were analyzed as described above.

Determination of 8-oxo-dG by HPLC-ECD. To detect oxidative DNA damage by •OH, we evaluated 8-oxo-dG by HPLC-ECD. Cells were suspended in RPMI 1640/10% FCS at 1×10^6/mL and exposed to 50 μM BT for 1, 2, or 4 hr; 20 μM HQ for 1 or 4 hr; or 20 μM CT for 2 hr, with all exposures at 37°C in 5% CO_2. The cells were immediately chilled in an ice-water bath, washed with ice-cold PBS, and then stored for later analysis as cell pellets at –80°C. DNA was extracted from the cells with DNA Extractor WB Kit (Wako Pure Chemical) according to the manufacturer's instructions and enzymatically digested to nucleosides, as described by Takeuchi et al. (1994). After HPLC separation, 8-oxo-dG was detected by ECD, and deoxyguanosine (dG) was detected by ultraviolet absorption as described elsewhere (Takeuchi et al. 1994). 8-oxo-dG level was expressed as the molar ratio of 8-oxo-dG per 10^5 dG.

Immunocytochemical detection of halogenated tyrosines. To detect protein damage by HOCl, we analyzed halogenated tyrosines using rabbit anti-chlorotyrosine antibody (Hycult Biotech, Uden, the Netherlands) (Gujral et al. 2003) and mouse anti-dibromotyrosine monoclonal antibody (JaiCA, Shizuoka, Japan), which cross-reacts with dichlorotyrosine (Kato et al. 2005). Cells were suspended in RPMI 1640/10% FCS at 4×10^5/mL and then exposed to 50 μM BT at 37°C in 5% CO_2 for 4 hr. After exposure, the cells were washed with PBS and centrifuged with Shandon Cytospin 4 (Thermo Scientific, Kanagawa, Japan) at 1,000 rpm for 8 min. Centrifuged cells on slides were dried and fixed with cold acetone and then blocked with PBS containing 2% bovine serum albumin. To detect chlorotyrosine, cells were incubated with anti-chlorotyrosine antibody and then stained with Alexa Fluor 488–conjugated goat anti-rabbit antibody (Invitrogen, Tokyo, Japan) and 1 μg/mL PI. To detect dibromo/dichlorotyrosine, cells were incubated with anti-dibromotyrosine antibody and then stained with Alexa Fluor 488–conjugated goat anti-mouse antibody and 1 μg/mL PI. The stained slides were examined by fluorescence microscopy.

Statistical analysis. Data are presented as mean + SE. Statistical analyses were performed using PASW Statistics software (version 18.0; SPSS, Inc., Tokyo, Japan). Treatment effects were established by nonparametric Wilcoxon tests. Data for DNA damage were analyzed using analysis of variance, followed by Fisher's protected least significant difference test for post hoc comparisons of individual treatments. p-Values < 0.05 (two tailed) were considered significant.

Results

Levels of apoptosis and intracellular ROS after BT exposure. We found more annexin V–positive and PI-negative cells, considered to be apoptotic, in HL-60 cells that had been exposed to 50 μM BT for 8 hr

(Figure 1B) than in controls (Figure 1A). The percentage of apoptotic cells in HL-60 cells exposed to 50 μM BT was significantly greater than in unexposed cells (Figure 1C, inset). Apoptosis increased depending on the concentration of BT (Figure 1C).

We determined intracellular ROS flow cytometrically using ROS-sensitive fluorescent probes: HE for $O_2^{\bullet-}$, DCFH-DA for H_2O_2, APF for HOCl, and HPF for $^{\bullet}OH$. BT increased the intracellular levels of each of these ROS (Figure 1D).

Effect of ROS scavengers and MPO inhibitor on apoptosis and intracellular ROS. Apoptosis was inhibited by catalase, ABAH, and methionine (Figure 2A). Catalase also inhibited the generation of $O_2^{\bullet-}$, H_2O_2, HOCl, and $^{\bullet}OH$ induced by BT exposure (Figure 2B). Although ABAH inhibited the BT-induced increase of HOCl and $^{\bullet}OH$, it further increased the generation of $O_2^{\bullet-}$ (Figure 2C). We could not determine the effect of ABAH on H_2O_2 because peroxidases, which are required for the conversion of DCFH to DCF, were inhibited by ABAH (Matsugo et al. 2006).

Levels of halogenated DNA. Using flow cytometry after immunostaining, we measured the level of halogenated DNA in HL-60 cells exposed to 50 μM BT. HL-60 cells exposed to BT for 1 hr showed about the same levels of halogenated DNA as control (unexposed) cells. However, after 4 hr exposure to BT, increased levels of halogenated DNA were apparent (Figure 3A,B). Although catalase, methionine, and ABAH inhibited these increases (Figure 3C), the levels of halogenated DNA were still higher than those in control cells. HL-60 cells exposed to 1 mM NaOCl for 1 hr and for 4 hr had significantly more halogenated DNA (Figure 3B). In contrast, exposure to HQ did not increase the level of halogenated DNA (Figure 3B).

Levels of 8-oxo-dG. Using HPLC-ECD, we measured 8-oxo-dG levels in HL-60 cells exposed to 50 μM BT, 20 μM HQ, or 20 μM CT. HL-60 cells exposed to 20 μM CT for 2 hr had significantly more 8-oxo-dG. However, BT and HQ had about the same 8-oxo-dG levels as the control cells (Figure 4).

Detection of halogenated tyrosines. To confirm the induction of halogenative stress in HL-60 cells by BT, we detected HOCl-induced protein damage in the form of halogenated tyrosines. After 4 hr exposure to 50 μM BT, levels of both chlorotyrosine (Figure 5A,B) and dibromo/dichlorotyrosine (Figure 5C,D) were elevated.

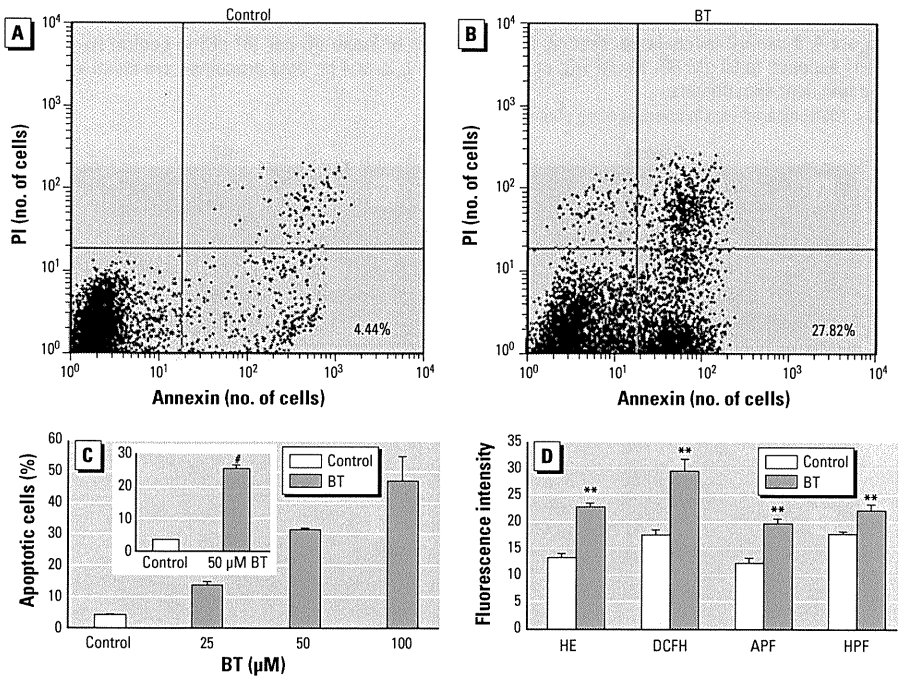

Figure 1. Apoptosis and intracellular ROS. (*A,B*) Representative dot graphs of unexposed HL-60 cells (control; *A*) and cells exposed to 50 μM BT for 8 hr (*B*). Cells in the lower right quadrant, which were stained with annexin V but not PI, were considered to be apoptotic; percentages of these cells in are shown in the figure. (*C*) Percentages of apoptotic HL-60 cells after exposure to BT for 8 hr; data presented are mean + SE from two independent experiments conducted in duplicate. Inset, percentages of apoptotic cells in controls or HL-60 cells exposed to 50 μM BT for 8 hr (mean + SE of 15 independent experiments conducted in duplicate). (*D*) Fluorescence intensities, corresponding to levels of various ROS, in controls or cells exposed to 50 μM BT for 30 min (mean + SE from 5–7 independent experiments conducted in duplicate). Fluorescence intensity is shown in arbitrary units.
$^{**}p < 0.01$, and $^{\#}p < 0.001$, compared with control.

Discussion

Because the findings of *in vivo* and *in vitro* research so strongly implicate the involvement of ROS in benzene-induced toxicity (Snyder and Hedli 1996), we designed a study to investigate the carcinogenic mechanism of benzene, focusing on BT, a benzene metabolite that generates ROS by autoxidation (Kawanishi et al. 1989; Zhang et al. 1996). We specifically examined the cytotoxic effects of BT on a human myeloid cell line, a class of cells from the organ mainly affected by benzene.

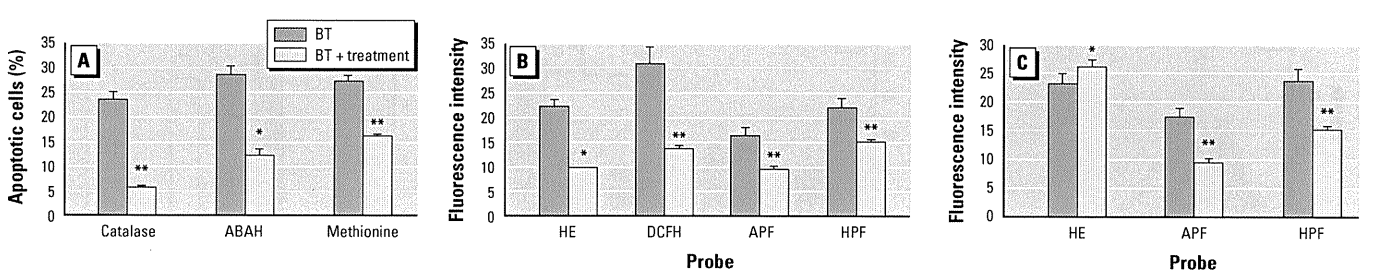

Figure 2. Suppression of BT-induced apoptosis and ROS generation by ROS scavengers (catalase and methionine) and an MPO inhibitor (ABAH). (*A*) Percentages of apoptotic cells in HL-60 exposed to 50 μM BT for 8 hr in the presence of MPO inhibitor and ROS scavengers; data presented are mean +SE from four to six independent experiments conducted in duplicate. (*B*) Effects of catalase on ROS generated by BT, as shown by fluorescence intensity of HE (for $O_2^{\bullet-}$), DCFH-DA (for H_2O_2), APF (for HOCl), and HPF (for $^{\bullet}OH$) in cells exposed to BT or BT plus catalase for 30 min (mean + SE from three to five independent experiments conducted in duplicate). (*C*) Effects of ABAH on ROS generated by BT, as shown by fluorescence intensity of HE, APF, and HPF in cells exposed for 30 min to BT or BT plus ABAH (mean + SE from three to five independent experiments conducted in duplicate).
$^{*}p < 0.05$, and $^{**}p < 0.01$ compared with the corresponding cells exposed to BT alone.

BT induced apoptosis in HL-60 cells in a concentration-dependent manner. Several ROS, including $O_2^{\bullet-}$, H_2O_2, HOCl, and $^{\bullet}OH$, were generated by exposure to 50 μM BT. The significant inhibition of BT-induced apoptosis in the presence of methionine, a relatively specific scavenger of HOCl (Tomono et al. 2009), suggests that BT generates HOCl. Moreover, BT exposure increased the amount of halogenated DNA and halogenated tyrosines detected by immunological examinations, which confirms generation of HOCl by BT. To the best of our knowledge, no previous studies have evaluated the generation of HOCl by benzene and its metabolites.

To investigate the mechanism of MPO-mediated apoptosis in HL-60 cells, we co-incubated HL-60 cells with BT and catalase or pretreated cells with ABAH or methionine, and then exposed them to BT. These reagents drastically suppressed the level of BT-induced apoptosis. This strongly implicates the H_2O_2–MPO–HOCl system in the induction of apoptosis by BT. Catalase inhibited BT-induced generation of ROS, and ABAH specifically inhibited BT-induced generation of HOCl and $^{\bullet}OH$. This inhibition indicates that HOCl was generated via the H_2O_2–MPO–HOCl system. The inhibition of HOCl generation by both catalase and ABAH demonstrates that, in HL-60 cells exposed to BT, H_2O_2 was certainly metabolized to HOCl by MPO. It also suggests that HOCl might trigger BT-induced apoptosis of HL-60 cells. In contrast, ABAH further increased the BT-induced generation of $O_2^{\bullet-}$, which indicates an accumulation of $O_2^{\bullet-}$ caused by the inhibition of MPO and also indicates that $O_2^{\bullet-}$ and probably H_2O_2 do not directly trigger apoptosis.

We then investigated whether this cytotoxicity of BT was related to the induction of DNA damage. We evaluated the halogenation of DNA by HOCl, and 8-oxo-dG induction by $^{\bullet}OH$. Although CT exposure increased 8-oxo-dG as previously reported (Oikawa et al. 2001), BT exposure did not. In HL-60 cells exposed to BT, however, we did detect more halogenated DNA. Furthermore, catalase, ABAH, and methionine clearly inhibited DNA halogenation. These findings indicate that HOCl was generated by MPO after BT exposure, and that this HOCl was the likely culprit in DNA halogenation. We also tested whether HQ induces DNA damage. However, 20 μM HQ did not increase either

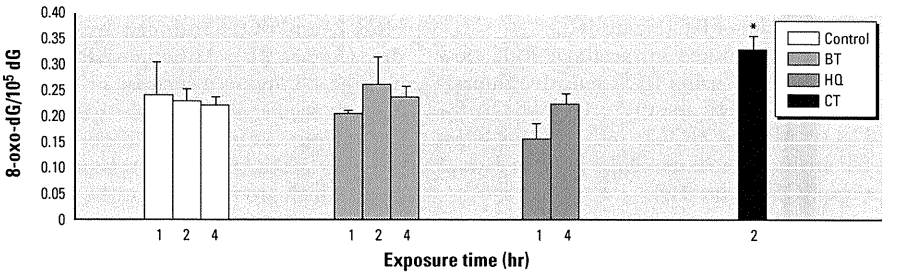

Figure 4. 8-oxo-dG levels (expressed as the molar ratio of 8-oxo-dG per 10^5 dG) in control HL-60 cells or cells exposed to 50 μM BT, 20 μM HQ, or 20 μM CT for 1, 2, or 4 hr; data presented are mean + SE of four independent experiments.
*$p < 0.05$ compared with in corresponding control.

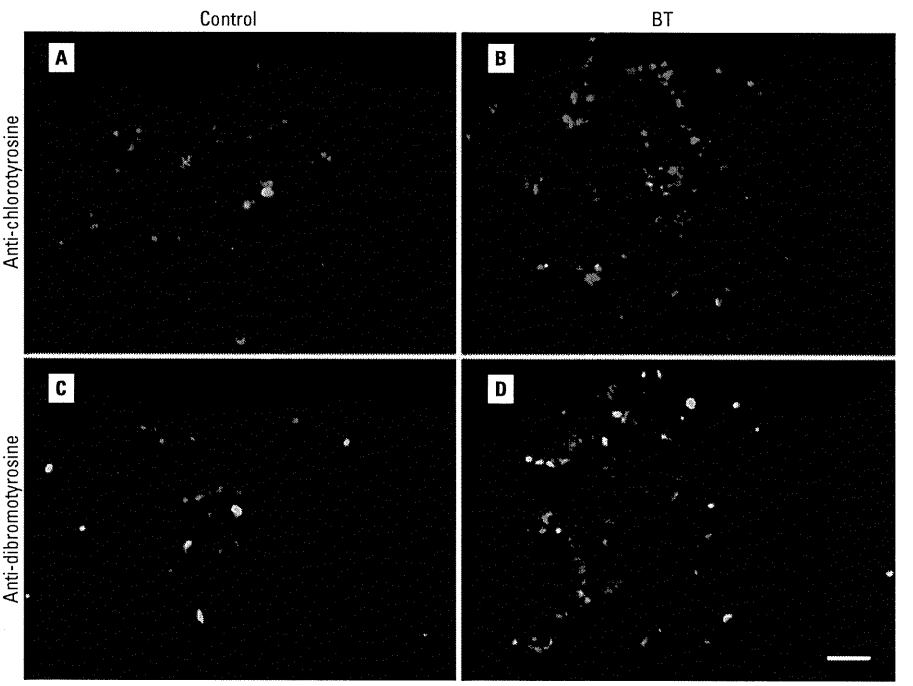

Figure 5. Halogenated tyrosines in unexposed (control) HL-60 cells (*A*, *C*) and cells exposed to 50 μM BT (*B*, *D*) stained with anti-chlorotyrosine antibody (*A*, *B*) or anti-dibromotyrosine antibody (*C*, *D*). See "Materials and Methods" for details. Green indicates halogenated tyrosines stained with Alexa Fluor 488; red indicates nucleic acids stained with PI. Magnification, 200×. Bar = 50 μm.

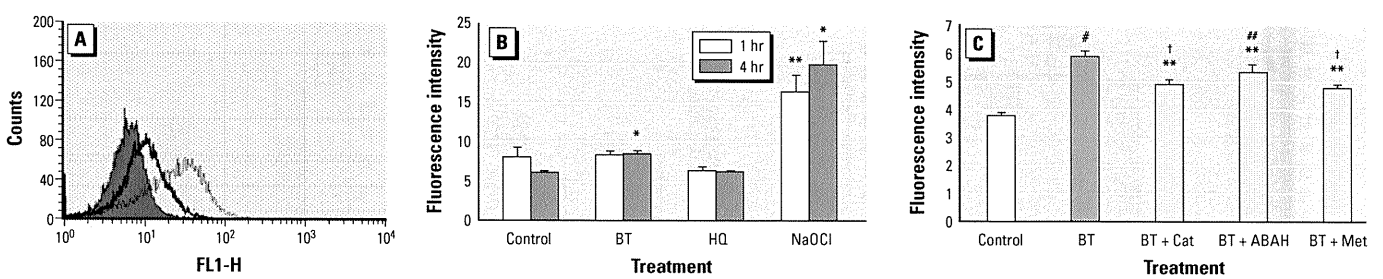

Figure 3. Induction of halogenated DNA in HL-60 cells by BT. (*A*) Histograms showing results for control HL-60 cells (gray shaded area) and cells exposed for 4 hr to 50 μM BT (black line) or 1 mM NaOCl (gray dotted line). FL1-H, height of green fluorescence. (*B*) Fluorescence intensities (arbitrary units) of controls or cells exposed to 50 μM BT, 20 μM HQ, or 1 mM NaOCl for 1 or 4 hr; data presented are mean + SE from 4 independent experiments conducted in duplicate. (*C*) Fluorescence intensities of controls or cells exposed for 4 hr to 50 μM BT, 50 μM BT with catalase (BT+Cat), 50 μM BT with ABAH (BT+ABAH), or 50 μM BT with methionine (BT+Met) (mean + SE of 3 independent experiments conducted in duplicate).
*$p < 0.05$ compared with the corresponding control. **$p < 0.01$, and $^{\#}p < 0.001$ compared with control. $^{\#\#}p < 0.05$, $^{\dagger}p < 0.01$ compared with the corresponding HL-60 cells that were exposed to BT alone.

the halogenated DNA or 8-oxo-dG. These results may help explain why HQ does not induce leukemia in humans (Levitt 2007). HQ is known to autoxidize more slowly and simply than does BT (Kawanishi et al. 1989), possibly accounting for the difference between BT and HQ; further study is required to confirm this.

Among halogenated nucleosides resulting from reaction with HOCl, 5-CldC, 5-chlorouracil, 8-chloro-deoxyadenine, and 8-chlorodeoxyguanine have been identified (Whiteman et al. 1997), with 5-CldC being the predominant carbon-chlorinated nucleoside product (Henderson et al. 1999). The mAb2D3 monoclonal antibody that we used in this experiment recognizes mainly 5-CldC (Kawai et al. 2004, 2008). Exposing DNA to HOCl causes large increases in pyrimidine oxidation, with no evidence of purine oxidation (i.e., 8-oxo-dG) (Whiteman et al. 1997). This effect is consistent with our finding of halogen-damaged DNA, such as 5-CldC, and no evidence of increased 8-oxo-dG. In contrast, exposing DNA to HOCl has been reported to increase the 8-oxo-dG level (Ohnishi et al. 2002); however, that finding may have been due to the addition of diethylenetriaminepentaacetic acid to the reaction mixture. In another study, Kolachana et al. (1993) reported the induction of 8-oxo-dG in HL-60 cells by BT. The discrepancy between our results and those of that study may be explained by the difference in the precision of HPLC-ECD methods. In unexposed cells, we detected levels of 8-oxo-dG about 0.2 per 10^5 dG. By contrast, assuming that the average molecular weight of nucleotides is 300, the 8-oxo-dG level in the other report was about 9.6 per 10^5 dG.

Oxidative DNA damage has been implicated in carcinogenesis (Weitzman and Gordon 1990). Although normal cells are able to efficiently repair the products of most promutagenic HOCl-mediated damage, no repair activity has been identified for 5-chlorocytosine, probably because 5-chlorocytosine mimics 5-methylcytosine (Lao et al. 2009). The presence of 5-chlorocytosine, which can be misrecognized by cellular machinery as 5-methylcytosine, would alter methylation patterns. In addition, 5-chlorocytosine is easily transformed to 5-chlorouracil (Theruvathu et al. 2009). Because 5-chlorouracil residues can pair with adenine as well as guanine (Kim et al. 2010), 5-chlorouracil–adenine base pairing might induce genetic mutation. Consequently, halogenated DNA is potentially able to induce both epigenetic and genetic changes that contribute to carcinogenesis.

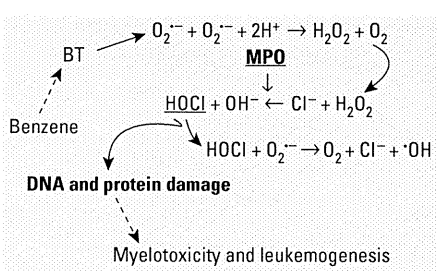

Figure 6. Hypothesized mechanism of cytotoxicity of BT involved in myelotoxicity and leukemogenesis of benzene.

Inoue et al. (1989) detected BT in human urine after benzene exposure; the urinary concentration of BT linearly correlated with the degree of benzene exposure, reaching > 50 mg/L (396 μM) in a worker exposed to 210 ppm benzene. In addition, Aksoy (1989) reported on Turkish workers who were chronically exposed to up to 650 ppm benzene, some of whom developed leukemia. We believe that it is plausible that 50 μM BT, the concentration used in the present study, could have been present in the workers.

Individuals with *MPO* polymorphism –463G→A in the promoter region, which reduces MPO expression, have decreased risk for various cancers (Cascorbi et al. 2000). Lan et al. (2004) reported that benzene-exposed workers with the –463G genotype showed greater hematotoxicity than did workers with the –463A genotype. These findings suggest important roles in myelotoxicity or carcinogenesis for MPO-catalyzed reactions toward HOCl.

In the present study we have constructed a novel hypothesis (Figure 6) that exposure to BT increases $O_2^{\cdot-}$ generation, possibly by autoxidation. The $O_2^{\cdot-}$ is chemically or enzymatically converted to H_2O_2, which is then metabolized to HOCl by MPO; this HOCl halogenates DNA and proteins, thus inducing myelotoxicity or leukemogenesis. The high expression of MPO from myeloid cells, along with the fact that halogenated DNA can cause gene mutation and epigenetic changes, may explain how benzene is involved in bone marrow disorders or myeloid leukemia. A previous study of benzene toxicity reported that MPO plays a role in the bioactivation of benzene's phenolic metabolites (Eastmond et al. 2005). Here, we show for the first time that a benzene metabolite, BT, is capable of generating HOCl and consequent halogenative damage via the H_2O_2–MPO–HOCl system. Our findings lend strong support to the hypothesis that BT-induced DNA halogenation is a primary reaction in leukemogenesis associated with benzene.

References

Aksoy M. 1989. Hematotoxicity and carcinogenicity of benzene. Environ Health Perspect 82:193–197.

Cascorbi I, Henning S, Brockmöller J, Gephart J, Meisel C, Müller JM, et al. 2000. Substantially reduced risk of cancer of the aerodigestive tract in subjects with variant –463A of the myeloperoxidase gene. Cancer Res 60:644–649.

Eastmond DA, Mondrala ST, Hasegawa L. 2005. Topoisomerase II inhibition by myeloperoxidase-activated hydroquinone: a potential mechanism underlying the genotoxic and carcinogenic effects of benzene. Chem Biol Interact 153–154: 207–216.

Gujral JS, Farhood A, Bajt ML, Jaeschke H. 2003. Neutrophils aggravate acute liver injury during obstructive cholestasis in bile duct-ligated mice. Hepatology 38:355–363.

Heller JI, Crowley JR, Hazen SL, Salvay DM, Wagner P, Pennathur S, et al. 2000. *p*-Hydroxyphenylacetaldehyde, an aldehyde generated by myeloperoxidase, modifies phospholipid amino groups of low density lipoprotein in human atherosclerotic intima. J Biol Chem 275:9957–9962.

Henderson JP, Byun J, Heinecke JW. 1999. Molecular chlorine generated by the myeloperoxidase-hydrogen peroxide-chloride system of phagocytes produces 5-chlorocytosine in bacterial RNA. J Biol Chem 274:33440–33448.

Henderson RF, Sabourin PJ, Bechtold WE, Griffith WC, Medinsky MA, Birnbaum LS, et al. 1989. The effect of dose, dose rate, route of administration, and species on tissue and blood levels of benzene metabolites. Environ Health Perspect 82:9–17.

Huff J. 2007. Benzene-induced cancers: abridged history and occupational health impact. Int J Occup Environ Health 13:213–221.

Hurst JK, Barrette WC Jr. 1989. Leukocytic oxygen activation and microbicidal oxidative toxins. Crit Rev Biochem Mol Biol 24:271–328.

IARC (International Agency for Research on Cancer). 2011. Agents Classified by the *IARC Monographs*, Volumes 1–102. Available: http://monographs.iarc.fr/ENG/Classification/ClassificationsAlphaOrder.pdf [accessed 14 November 2011].

Inoue O, Seiji K, Nakatsuka H, Watanabe T, Yin S, Li GL, et al. 1989. Excretion of 1,2,4-benzenetriol in the urine of workers exposed to benzene. Br J Ind Med 46:559–565.

Kato Y, Kawai Y, Morinaga H, Kondo H, Dozaki N, Kitamoto N, et al. 2005. Immunogenicity of a brominated protein and successive establishment of a monoclonal antibody to dihalogenated tyrosine. Free Radic Biol Med 38:24–31.

Kawai Y, Matsui Y, Kondo H, Morinaga H, Uchida K, Miyoshi N, et al. 2008. Galloylated catechins as potent inhibitors of hypochlorous acid-induced DNA damage. Chem Res Toxicol 21:1407–1414.

Kawai Y, Morinaga H, Kondo H, Miyoshi N, Nakamura Y, Uchida K, et al. 2004. Endogeneous formation of novel halogenated 2′-deoxycytidine. Hypohalous acid-mediated DNA modification at the site of inflammation. J Biol Chem 279:51241–51249.

Kawanishi S, Inoue S, Kawanishi M. 1989. Human DNA damage induced by 1,2,4-benzenetriol, a benzene metabolite. Cancer Res 49:164–168.

Kim CH, Darwanto A, Theruvathu JA, Herring JL, Sowers LC. 2010. Polymerase incorporation and miscoding properties of 5-chlorouracil. Chem Res Toxicol 23:740–748.

Kohanski MA, Dwyer DJ, Hayete B, Lawrence CA, Collins JJ. 2007. A common mechanism of cellular death induced by bacterial antibiotics. Cell 130:797–810.

Kolachana P, Subrahmanyam VV, Meyer KB, Zhang L, Smith MT. 1993. Benzene and its phenolic metabolites produce oxidative DNA damage in HL60 cells *in vitro* and in the bone marrow *in vivo*. Cancer Res 53:1023–1026.

Lan Q, Zhang L, Li G, Vermeulen R, Weinberg RS, Dosemeci M, et al. 2004. Hematotoxicity in workers exposed to low levels of benzene. Science 306:1774–1776.

Lao VV, Herring JL, Kim CH, Darwanto A, Soto U, Sowers LC. 2009. Incorporation of 5-chlorocytosine into mammalian DNA results in heritable gene silencing and altered cytosine methylation patterns. Carcinogenesis 30:886–893.

Levitt J. 2007. The safety of hydroquinone: a dermatologist's response to the 2006 *Federal Register*. J Am Acad Dermatol 57:854–872.

Lewis JG, Stewart W, Adams DO. 1988. Role of oxygen radicals in induction of DNA damage by metabolites of benzene. Cancer Res 48:4762–4765.

Marnett LJ. 2000. Oxyradicals and DNA damage. Carcinogenesis 21:361–370.

Matsugo S, Sasai M, Shinmori H, Yasui F, Takeuchi M, Takeuchi T. 2006. Generation of a novel fluorescent product, monochlorofluorescein from dichlorofluorescin by photoirradiation. Free Radic Res 40:959–965.

Nakazato T, Sagawa M, Yamato K, Xian M, Yamamoto T, Suematsu M, et al. 2007. Myeloperoxidase is a key regulator of oxidative stress-mediated apoptosis in myeloid leukemic cells. Clin Cancer Res 13:5436–5443.

Ohnishi S, Murata M, Kawanishi S. 2002. DNA damage induced

by hypochlorite and hypobromite with reference to inflammation-associated carcinogenesis. Cancer Lett 178:37–42.
Oikawa S, Hirosawa I, Hirakawa K, Kawanishi S. 2001. Site specificity and mechanism of oxidative DNA damage induced by carcinogenic catechol. Carcinogenesis 22:1239–1245.
Rothe G, Valet G. 1990. Flow cytometric analysis of respiratory burst activity in phagocytes with hydroethidine and 2',7'-dichlorofluorescin. J Leukoc Biol 47:440–448.
Setsukinai K, Urano Y, Kakinuma K, Majima HJ, Nagano T. 2003. Development of novel fluorescence probes that can reliably detect reactive oxygen species and distinguish specific species. J Biol Chem 278:3170–3175.
Snyder R, Hedli CC. 1996. An overview of benzene metabolism. Environ Health Perspect 104(suppl 6):1165–1171.
Takeuchi T, Nakajima M, Morimoto K. 1996. Relationship between the intracellular reactive oxygen species and the induction of oxidative DNA damage in human neutrophil-like cells. Carcinogenesis 17:1543–1548.
Takeuchi T, Nakajima M, Ohta Y, Mure K, Takeshita T, Morimoto K. 1994. Evaluation of 8-hydroxydeoxyguanosine, a typical oxidative DNA damage, in human leukocytes. Carcinogenesis 15:1519–1523.
Theruvathu JA, Kim CH, Darwanto A, Neidigh JW, Sowers LC. 2009. pH-Dependent configurations of a 5-chlorouracil-guanine base pair. Biochemistry 48:11312–11318.
Tomono S, Miyoshi N, Sato K, Ohba Y, Ohshima H. 2009. Formation of cholesterol ozonolysis products through an ozone-free mechanism mediated by the myeloperoxidase-H_2O_2-chloride system. Biochem Biophys Res Commun 383:222–227.
Weitzman SA, Gordon LI. 1990. Inflammation and cancer: role of phagocyte-generated oxidants in carcinogenesis. Blood 76:655–663.
Whiteman M, Jenner A, Halliwell B. 1997. Hypochlorous acid-induced base modifications in isolated calf thymus DNA. Chem Res Toxicol 10:1240–1246.
Whysner J, Reddy MV, Ross PM, Mohan M, Lax EA. 2004. Genotoxicity of benzene and its metabolites. Mutat Res 566:99–130.
Zhang L, Bandy B, Davison AJ. 1996. Effects of metals, ligands and antioxidants on the reaction of oxygen with 1,2,4-benzenetriol. Free Radic Biol Med 20:495–505.

JJCO Japanese Journal of Clinical Oncology

Short Communication

Jpn J Clin Oncol 2011;41(6)820–824
doi:10.1093/jjco/hyr029
Advance Access Publication 16 March 2011

Administration Schedule of Daunorubicin for Elderly Patients with Acute Myelogenous Leukemia: A Single-institute Experience

Nobuaki Dobashi[1,2,*], Noriko Usui[1,2], Shingo Yano[1], Yuichi Yahagi[1], Yutaka Takei[1,2], Katsuki Sugiyama[1], Shinobu Takahara[1], Yoji Ogasawara[1], Yuko Yamaguchi[1,2], Takeshi Saito[1], Hiroki Yokoyama[1,2] and Keisuke Aiba[1]

[1]Division of Clinical Oncology and Hematology, Department of Internal Medicine, Jikei University School of Medicine and [2]Department of Clinical Oncology and Hematology, Jikei University Daisan Hospital, Tokyo, Japan

*For reprints and all correspondence: Nobuaki Dobashi, Department of Clinical Oncology and Hematology, Jikei University Daisan Hospital, 4-11-1, Izumi-honcho, Komae-shi, Tokyo 201-8601, Japan. E-mail: dobashi@jikei.ac.jp

Received October 21, 2010; accepted February 13, 2011

We evaluated the efficacy of daunorubicin (40 mg/m^2/day for 5 days, 200 mg/m^2/cycle) combined with standard dose of cytarabine (100 mg/m^2/day for 7 days) for acute myelogenous leukemia patients aged 65–74 years as induction therapy. Complete remission (81.3%) was achieved in 13 of 16 patients following the therapeutic program. The median duration of recovering absolute neutolophilic counts over 1000/μl and platelet counts over 100 000/μl were 33 days and 27 days, respectively. None of the patients had any adverse cardiac complications or died during administration of the induction therapy. Patients achieving complete remission received post-remission therapy consisting of two regimens other than induction therapy. The 3-year disease-free and overall survival rates were 36.9 and 50.0%, respectively. Extending the total period of the daunorubicin therapy might be an alternative to increasing the daily dose of daunorubicin in the induction therapy for elderly patients who were candidates for receiving intensified chemotherapy.

Key words: elderly patients – AML – intensified DNR – induction therapy

INTRODUCTION

Advances in the treatment for acute myelogenous leukemia (AML) have been obtained with intensified approaches and development of novel agents. In elderly AML patients who were judged by physicians to be fit for intensive chemotherapy, standard therapy such as '3 + 7' [3 days of daunorubicin (DNR) and 7 days of cytarabine at conventional dose] or intensive investigational therapy are usually employed (1–3). However, the most appropriate chemotherapy for elderly AML patients is still controversial due to both biological disease-related and patient-specific factors (4–6). There is an urgent need to find innovative treatments for elderly AML patients. We previously reported two studies on intensified DNR in induction therapy for adult AML patients younger than 65 years (7,8). To increase the intensity of induction therapy, we administrated DNR (40 mg/m^2/day) by expanding the total period of infusion more than 3 days instead of increasing daily dose of DNR in these two studies. On the basis of our institution's experience, we administered DNR (40 mg/m^2/day for 5 days, 200 mg/m^2/cycle) combined with cytarabine (100 mg/m^2/day for 7 days) to previously untreated AML patients aged 65–74 years as induction therapy. Here, we conducted retrospective analysis of the clinical outcome of elderly AML patients treated by extending the total period of DNR combined with cytarabine in induction therapy.

PATIENTS AND METHODS

Patients

Between January 2003 and March 2008, 21 untreated AML patients aged 65–74 years, except previously diagnosed myelodysplastic syndrome were admitted to our institution. Of the 21 patients, 4 patients did not undergo the therapeutic program because of their comorbid conditions (cerebral hemorrhage, senile dementia, uncontrolled diabetes mellitus and active double cancer). One patient refused receiving

intensive chemotherapy. Thus, 16 patients (76.2%) were enrolled in the therapeutic program.

Treatment Protocol

The dose and schedule of induction therapy were as follows: DNR was administered intravenously (IV) at a dose of 40 mg/m^2/day for 5 days, and cytarabine was administered continuous intravenously (CIV) at a dose of 100 mg/m^2/day for 7 days. When bone marrow (BM) examination revealed sufficient hypoplastic marrow (cellularity < 10 000 cells/μl) and M1 marrow (<5% blasts) at 4 days after initiating therapy, the administration of DNR was discontinued. If complete remission (CR) was not attained by the first cycle of treatment, 40 mg/m^2/day of DNR for 3 days and 100 mg/m^2/day of cytarabine for 7 days were administrated as the second cycle. The post-remission therapy was administered as follows: one cycle of DNR (40 mg/m^2/day IV for 3 days) combined with cytarabine (100 mg/m^2/day CIV for 7 days), two cycles of behenoyl cytarabine (170 mg/m^2/day IV for 7 days) combined with aclarubicin (17 mg/m^2/day IV for 7 days) and two cycles of mitoxantrone (10 mg/m^2/day IV for 1 day) combined with etoposide (200 mg/body/day orally for 5 days) and cytarabine (80 mg/m^2/day subcutaneous injected for 5 days).

Response Criteria and Statistical Analysis

CR was defined as the normalization of peripheral blood count and <5% blasts in the BM with normal cellularity. Relapse was defined as the reappearance of leukemic cells in the BM (>5% blasts) and/or reappearance of clinical evidence of the disease. Non-hematologic toxicity was graded according to the National Cancer Institute's Common Toxicity Criteria (version 3.0).The duration of disease-free survival (DFS) of a patient was measured from the first documentation of achievement of CR to the date of either the first incidence of relapse or death, and overall survival (OS) of a patient was measured from the time of initiation of the induction therapy to the death of the patient from any cause. DFS and OS distributions were computed with the Kaplan–Meier product limit estimator. The difference in DFS and OS between subgroups was evaluated by means of the log-rank test.

RESULTS

Patient Characteristics

The characteristics of the patients and their response to induction therapy are outlined in Table 1. All patients provided their written informed consent. Their median age was 70 years. Of the 10 patients with a normal karyotype, 7 patients were tested for FMS-like tyrosine kinase 3 (FLT3)-internal tandem duplication (ITD) by a semiquantitative polymerase chain reaction assay; the FLT3-ITD mutation was detected in only one patient. Nucleophosmin (*NPM1*) gene status was not tested in those patients. The median follow-up period for seven patients who were still alive at the date of last contact was 54.9 months.

Response to Induction Therapy and Survival

CR (81.3%; 95% confidence interval: 54.4–96.0%) was achieved in 13 patients; 4 of the 13 patients received a second cycle of the induction therapy. One patient, who did not achieve CR after the first cycle of the induction therapy, refused further treatment. The median percentage of BM blasts at day 4 of the therapy was 30.4% (range: 2–84.2). Only two patients were administered DNR for 3 days because their BM examination showed sufficient degree of hypoplasia at day 4 of the treatment. With regard to the hematologic changes resulting from the induction therapy, the median durations for recovery of the absolute neutrophil count to over 1000/μl and the platelet count to over 100 000/μl were 33 days (range: 19–37+) and 27 days (range: 21–39+), respectively. The major non-hematologic toxicities (grade: >2) were infection (92%), diarrhea (25%), mucositis (19%) and hepatotoxicity (13%). Granulocyte colony-stimulating factor was administered to four patients, because of complication of the documented infection. None of the patients had any adverse cardiac complications (grade: >2), and the median percentages of the left ventricular ejection fraction, measured by echocardiography, were 68% (range: 61–79) after receiving the induction therapy and 67% (range: 59–80) before initiation of the treatment.

The 13 patients who had achieved CR underwent the post-remission therapy. During this post-remission therapy, three patients relapsed and one patient died of pneumonia. After the post-remission therapy, four patients relapsed. Five patients maintained first CR at the date of this analysis. The 3-year DFS and OS rates were 36.9% (95% CI: 12.5–62.0%) and 50.0% (95% CI, 24.5–71.1%), respectively (Fig. 1A and B). Comparison of the outcomes between the favorable/normal karyotype group and the unfavorable karyotype group was made with regard to DFS and OS rates. There was no significant difference in those groups ($P = 0.749$ in DFS rate, $P = 0.331$ in OS rate) (Fig. 1C and D).

On the other hand, the clinical outcome of five patients who did not undergo the therapeutic program were as follows: three patients were treated with less intensive chemotherapy (DNR, 40 mg/m^2/day IV for 1 day, combined with cytarabine); however, they died of leukemia at 2, 6, 24 months after initiating the treatments, respectively. Two patients moved in other hospitals, and we lost their follow-up data.

DISCUSSION

The current report describes the response of 16 elderly patients to the induction therapy with a combination of DNR (administered for 5 days) and standard dose of cytarabine.